Virtually identical does not mean exactly identical: Discrepancy in energy metabolism between glucose and fructose fermentation influences the reproductive potential of yeast cells

Roman Maslanka*, Sabina Bednarska, Renata Zadrag-Tecza

Institute of Biology, College of Natural Sciences, University of Rzeszow, Rzeszow, Poland

*Corresponding author

Institute of Biology,

College of Natural Sciences, University of Rzeszow,

Zelwerowicza 4, 35-601 Rzeszow, Poland

Tel. +48177855413

E-mail: rmaslanka@ur.edu.pl

ABSTRACT

The physiological efficiency of cells largely depends on the possibility of metabolic adaptations to changing conditions, especially on the availability of nutrients. Central carbon metabolism has an essential role in cellular function. In most cells is based on glucose, which is the primary energy source, provides the carbon skeleton for the biosynthesis of important cell macromolecules, and acts as a signalling molecule. The metabolic flux between pathways of carbon metabolism such as glycolysis, pentose phosphate pathway, and mitochondrial oxidative phosphorylation is dynamically adjusted by specific cellular economics responding to extracellular conditions and intracellular demands. Using *Saccharomyces cerevisiae* yeast cells and potentially similar fermentable carbon sources i.e. glucose and fructose we analyzed the parameters concerning the metabolic status of the cells and connected with them alteration in cell reproductive potential. Those parameters were related to the specific metabolic network: the hexose uptake - glycolysis and activity of the cAMP/PKA pathway - pentose phosphate pathway and biosynthetic capacities - the oxidative respiration and energy generation. The results showed that yeast cells growing in a fructose medium slightly increased metabolism redirection toward respiratory activity, which decreased pentose phosphate pathway activity and cellular biosynthetic capabilities. These differences between the fermentative metabolism of glucose and fructose, lead to long-term effects, manifested by changes in the maximum reproductive potential of cells.

Keywords: fructose vs glucose, reproductive potential, cellular metabolism, mitochondrial respiration, carbon catabolite repression, hexokinase,

INTRODUCTION

Central carbon metabolism (CCM) has an essential role in cellular function and in the case of most cells is based on glucose, which is the primary source of energy. However, glucose provides also the carbon skeleton for biosynthesis and acts as a signaling molecule [1, 2]. Thus, carbon metabolism involves a network of interrelated pathways that provide energy, precursors for biosynthesis, and cofactors used in redox reactions. Those pathways are glycolysis, pentose phosphate pathway (PPP), and mitochondrial oxidative phosphorylation. The metabolic flux between them is found to be dynamically adjusted by specific cellular economics responding to extracellular conditions and intracellular demands [2-6]. Moreover, the metabolic trade-off between different types of glucose utilization can be also connected with specific growth strategies, stress conditions, or ecological niches [7-10]. Because glycolysis and oxidative phosphorylation are interconnected through thermodynamic and kinetic dependencies [11], there are many studies explaining the difference between oxidative respiration and fermentation [12-14]. However, nowadays more and more research shows that cell growth rate optimization seems to be connected with gradual metabolic shifts between the different pathways of energy generation, e.g.: (i) higher glycolytic flux is connected with shifting the metabolism from energetically efficient respiration to respiro-fermentative metabolism [15]; (ii) the switch toward respiration begins even when glucose is still available in the medium [16]; (iii) aerobic glycolysis does not have to fully replace the respiration and both processes can occur in parallel to support the metabolite needs of the cells [17]. Understanding the reversibly regulation between cellular bioenergetics pathways is crucial considering the metabolic phenomenon of enhanced aerobic glycolysis performed by highly proliferating cells, including cancer cells – Warburg effect [2, 18, 19], stem cells [4, 20], and budding yeast – Crabtree effect [21, 22].

The preference for less energy-efficient fermentative metabolism in the case of *Saccharomyces cerevisiae* yeast is connected with glucose-mediated repression of genes important for respiratory activity [23]. Since glucose acts as a metabolism-modulating molecule, its availability has to be constantly monitored by glucose-signaling pathways such as the RAS/cAMP/PKA signaling pathway [23-26]. Synthesis of cAMP depends on the G-protein coupled receptor (GPCR) system [25] but also can be stimulated by intracellular glucose catabolism required for activation of Ras proteins [26]. An important role in glycolytic flux and determination of the intracellular level of glucose play hexokinase 2 − Hxk2p. Hxk2p, Hxk1p (hexokinase 1), and Glk1p (glucokinase) are three isoenzymes with the hexokinase activity present in *S. cerevisiae*. When glucose is present in the medium, Hxk2p besides acting as a glycolytic enzyme, in cooperation with Mig1p, Mig2p, Reg1p, and Snf1p, forms a repressor

complex that bound to the *SUC2* promoter and represses the expression of several genes. The repressed genes include genes of high-affinity glucose transporters, genes involved in the utilization of alternative carbon sources, and genes responsible for the mitochondrial activity and respiratory metabolism [25, 27]. Moreover, Hxk2p (in conditions of high glucose level) repress also the expression of the *HXK1* and *GLK1* genes [28]. Therefore, the role of hexokinase 2 in glucose metabolism is the reason that Δ*hxk2* strain is regarded as a genetic model that mimics calorie restriction (CR) [29, 30].

Although, glucose metabolism seems to be quite well understood the issue concerning metabolic flux and the mechanism of cooperation between pathways composing the CCM is still an urgent topic for scientists. Our previous works showed that high glucose concentration (calorie excess – CE) and related changes in metabolic fluxes increase the biosynthetic capabilities and size of the yeast cells, but at the same time reduce their reproductive potential [30-32]. But otherwise, reduced PKA-activity and associated changes in CCM increase the reproductive potential of the yeast cells and can inhibit the negative consequences of CE [30, 32]. Besides glucose, also fructose is an easily fermented carbon source for yeast cells. Although fructose fermentation is regarded as similar to glucose fermentation the molecular mechanism and cause of preferential utilization of glucose over fructose are not fully understood. It is assumed that the discrepancy in glucose/fructose fermentation seems to be connected with the differential transport rate of those sugars and hexose transporters affinities [33-35] and/or differences in hexokinase kinetic properties and rate of hexose phosphorylation inside the cell [34-36]. There are very few conclusive analyses of the cellular mechanism of fructose action in the case of yeast [37, 38]. Moreover, according to the authors' knowledge, there are currently no studies comprehensively comparing the energetic and biosynthetic metabolism between glucose and fructose fermentation and simultaneously their influence on cell physiology and the reproductive potential of yeast cells.

This study aimed to investigate the effect of fructose utilization on the metabolic status, growth, and reproductive potential of yeast cells. The studies were conducted using WT and Δ*hxk2* yeast strains cultured on media with the same concentration of glucose or fructose. The experimental approach made it possible to explain interconnected changes in CCM and the role of metabolic adaptations in the regulation of the reproductive potential of the cells. The results of this work provide explanations about the differences between intracellular glucose and fructose metabolism, which may help understand the molecular aspects of fructose metabolism and its influence on certain aspects of human health, but also can be important in the context of undesirable aspects of fructose fermentation in industrial bioprocesses and wine production.

MATERIALS AND METHODS

Chemicals

6-(N-(7-nitrobenz-2-oxa-1,3-diazol-4-yl)amino)-6-deoxyglucose (6-NBDG); Dihydroethidium (DHET); rhodamine B hexyl ester were from Molecular Probes (Eugene, OR). BacTiter-Glo™ Microbial Cell Viability was from Promega (Madison, WI, USA). Antimycin A from *Streptomyces sp*., CAS number 1397-94-0; Oligomycin from *Streptomyces diastatochromogenes*, CAS number 1404-19-9; Glucose-6-Phosphate Assay Kit and ADP/ATP Ratio Assay Kit were from Sigma-Aldrich (St. Louis, MO, USA). 10 kDa MWCO spin Pierce Concentrator and Coomassie Protein Assay Reagent were from Thermo Scientific (Waltham, MA, USA). Direct cAMP Elisa Kit from Enzo Life Sciences (Lausen, Switzerland). GeneMATRIX Universal RNA Purification Kit was from EURx, (Gdańsk, Poland). Transcriptor First Strand cDNA Synthesis Kit; FastStart Essential DNA Probe Master and FastStart Essential DNA Green Master were from Roche (Mannheim, Germany). The probes for *ZWF1*, *HXT1*, and *ACT1* TaqMan™ Gene Expression Assay were from Applied Biosystems (Life Technologies, Pleasanton, CA, USA). Primers for *HXT6* and *ACT1* genes were prepared by Genomed (Warszawa, Poland). All other reagents were purchased from Sigma-Aldrich (Poznan, Poland). Components of culture media were from BD Difco (Becton Dickinson and Company, Spark, USA) except for glucose (POCH, Gliwice, Poland) and fructose (AppliChem, Darmstadt, Germany).

Yeast strains and growth conditions

The *S. cerevisiae* strains used in this study were all derivatives of BY4741. The wild-type (WT) BY4741 *MAT*a *his3 leu2 met15 ura3* and mutant strain Δ*hxk2 MAT*a *his3 leu2 met15 ura3 YGL253W::kanMX4* were from EUROSCARF yeast collection. The fluorescent GFP-tagged strains: Hxt1-GFP *MAT*a *his3 leu2 met15 ura3 HXT1-GFP::HIS3MX6* originate from yeast GFP clone collection [39]; Hxt6-GFP *MAT*a *his3 leu2 met15 ura3 HXT6-GFP::HIS3MX6* and Zwf1-GFP *MAT*a *his3 leu2 met15 ura3 ZWF1-GFP::HIS3MX6* were from the commercial Invitrogen Yeast GFP Clone Collection. Yeast cells were grown at 28°C in the liquid YP medium (1% Yeast Extract, 1% Yeast Bacto-Peptone) with different carbon sources (2% glucose and 2% fructose) on a rotary shaker at 150 rpm.

Determination of cell reproductive potential

The reproductive potential of yeast cells was determined by a routine procedure [40] on cells placed on agar plates using a micromanipulator, with modifications described in [41]. One-microliter aliquots of overnight yeast cultures grown on a YPD liquid medium with a specified

carbon source (2% glucose or 2% fructose) were dropped on YPD plates with a solid medium containing 2% glucose or 2% fructose, respectively. For each experiment, 40 single cells were micromanipulated to the appointed area. The first daughters were chosen as the starting cells, and their successive buddings were followed to determine the reproductive potential. During the manipulation, the plates were kept at 28°C for 16 h and at 4°C during the night. The data represent mean values from two separate experiments. The values of reproductive potential were also presented as violin plots which are a graphic representation of the distribution of that parameter in the analyzed population of cells. Maximum reproductive potential was calculated from 10% of cells with the highest number of daughters. Literature data inspired the introduction of such calculation which seems to be a useful indicator in lifespan research [42, 43].

Determination of cell growth and cell number in the culture

The growth of yeast cells was analyzed in the liquid medium. Yeast cultures were cultivated for 36 h in a shaking incubator (Heidolph incubator 1000) at 1200 rpm at 28°C. The growth was monitored turbidimetrically at λ = 600 nm using an Anthos 2010 type 17 550 microplate reader. Measurements were performed at 1 h intervals for 12 h and after 24 h and 48 h of cultivation. The growth rate was calculated from the exponential phase of growth using an appropriate formula [44]. The cell density (number of cells per ml) was determined using the Malassez chamber.

Bioimaging and fluorescence detection of yeast cells carrying GFP-tagged proteins

Cells carrying GFP-proteins (Hxt1-GFP; Hxt6-GFP; Zwf1-GFP) were cultured in a YPD medium with 2% glucose or 2% fructose for a specified time and growth phase (exponential, stationary, and 2 days). The cell number and carbohydrate concentration in the medium at each time were evaluated and compared between growth conditions. In each time the same number of yeast cells was harvested by centrifugation, washed twice with sterile PBS pH 7.4 buffer, and suspended to a final density of 10^8 cells/mL in the same buffer. Immediately the GFP fluorescence of the cell suspension was measured using a microplate reader Infinite 200 (Tecan Group Ltd., Männedorf, Switzerland) at λ_{ex} = 470 nm and λ_{em} = 510 nm. The location of each analyzed protein was also visualized using fluorescence microscopy at appropriate for GFP fluorescence wavelengths. The microscopic images, which present typical results of the duplicate experiment, were captured at 1000× magnification with the Olympus BX-51 microscope (Olympus, Tokyo, Japan) equipped with the DP-72 digital camera and cellSens Dimension v1.0 software.

Determination of carbohydrate concentration in media

Quantitative determination of glucose or fructose concentration was performed with copper and arsenolmolybdate reagents by the Somogyi-Nelson method. The method's principle involves forming cuprous oxide while heating copper reagent with the reducing sugar (glucose or fructose). The amount of copper oxide (I) is determined using the arsenomolybdate reagent, which is reduced to molybdenum blue and can be measured spectrophotometrically. The absorbance intensity is proportional to the amount of Cu_2O and therefore the amount of glucose or fructose in the analyzed sample.

Yeast cells were grown in YPD media with 2% glucose or 2% fructose for the time required for the studies (i.e. 12; 16; 20; 24 h or culture time of yeast cells carrying GFP-tagged proteins). After the specified culture time the cell suspensions were centrifuged and the concentration of glucose or fructose was determined in the culture medium after the removal of the yeast cells. Samples of media were diluted 100-fold to the volume of 0.5 mL; afterward, 0.5 mL of alkaline copper reagent was added to the samples and placed in a boiling water bath for 20 minutes. After cooling, 0.5 mL of arsenomolybdate reagent was added to the samples. Then the volume of the mixture was increased to 5 mL by adding water. The absorbance of the samples was measured at λ = 520 nm. Carbohydrate content was calculated from a standard curve made for samples with known concentrations of glucose or fructose, independently.

Measurement of glucose uptake

The glucose uptake rate was determined by using 6-NDBG, a fluorescent non-hydrolyzable glucose analog as described previously [31]. Cells from the early exponential phase of growth were washed and suspended in sterile phosphate-buffered saline (PBS) with pH 7.4. 6-NBDG was added to the cell suspension at the final concentration of 150 μM. Cells were incubated at 28°C for 90 min. After incubation, the reaction was stopped by twice washing the cells with PBS. The fluorescence of the cells was recorded using a microplate reader Infinite 200 at λ_{ex} = 455 nm and λ_{em} = 540 nm.

RNA Samples

RNA samples were obtained using GeneMATRIX Universal RNA Purification Kit according to the manufacturer's protocol (EURx, Gdańsk, Poland). Cells from the exponential phase of the culture (5×10^7 cells/mL) were centrifuged, washed twice with sterile water, and suspended in the spheroplast buffer (1 M sorbitol, 0.1 M EDTA, 0.1% β-mercaptoethanol) containing lyticase (250 U per sample) for 30 min at 30°C. The resultant spheroplasts were used for RNA isolation. RNA samples were stored at −20°C, and each of them was thawed only once. The

concentration and purity of RNA samples were measured with a microplate reader Infinite 200 equipped with a NanoQuant Plate using a 260 nm/280 nm ratio.

Quantitative Real-Time PCR

A total of 500 ng of RNA previously treated with DNase I (Roche) for 60 min, 25 °C (10 U per 1 μg RNA) was used for reverse transcription. To synthesize cDNA, Transcriptor First Strand cDNA Synthesis Kit (Roche) was applied according to the manufacturer's protocol, and the samples were stored at −50 °C until use. Real-time PCR was performed using LightCycler® 96 (Roche, Mannheim, Germany) equipment and TaqMan or SYBR Green chemistry. The *HXT1* and *ZWF1* gene expression level was tested by TaqMan chemistry. Briefly, the cDNA sample was diluted and mixed with FastStart Essential DNA Probe Master (Roche) and TaqMan Gene Expression Assays (Applied Biosystems, Life Technologies). A PCR reaction was performed for independent biological replicates. The *HXT6* gene expression level was tested by SYBR Green chemistry. Briefly, the cDNA sample was diluted and mixed with FastStart Essential DNA Green Master (Roche) and oligonucleotide primers dissolved in TE buffer pH 8 (10mM Tris-HCl; 1mM EDTA) to a concentration of 10 μM. A PCR reaction was performed for independent biological replicates. Primer sequences were: *HXT6*: forward 5′- CTA TGC TTC CGT GGG TGT CA-3′, reverse 5′- ACA GTT ACC AGC ACC CTT GG-3′; *ACT1*: forward 5′- AAT CAC CGC TTT GGC TCC AT-3′, reverse 5′- AGA ACC ACC AAT CCA GAC GG-3′. In both types of gene expression assays *ACT1* gene was used as an internal control. The efficiency of the SYBR Green RT-PCR reaction was evaluated by running a set of 10-fold dilutions of cDNA template. The relative gene expression was calculated with the $-\Delta C_T$ method for comparison of individual gene expression in tested conditions and yeast strains.

Preparation of cell extracts

The yeast cells from the exponential phase of growth were centrifuged, washed twice with sterile water, and suspended in cold homogenization buffer (20 mM phosphate buffer with pH 6.8, containing 1 mM EDTA and 1 mM PMSF). The cells were disrupted with 0.5 mm glass beads, vortexed in 7 cycles for 30 s with intervals for cooling the sample on ice, and then centrifuged (14 000× g, 15 min, 4°C). Supernatants were transferred to new tubes and immediately frozen at −80°C. The supernatants were used for the determination of protein content, pentose phosphate pathway enzyme activity, and glucose-6-phosphate content in the yeast cell.

Determination of protein content in the yeast cell

Protein concentration was determined using the Bradford method. The absorbance of samples was measured after 10 minutes of incubation with Coomassie Protein Assay Reagent (Thermo Scientific, Waltham, MA, USA) at room temperature using a microplate reader Infinite 200 at λ = 595 nm. The data were expressed as mg per mL, but also protein content per single cell was calculated.

Determination of glucose-6-phosphate content in the yeast cell

The level of glucose-6-phosphate in yeast cells was determined with Glucose-6-Phosphate Assay according to the manufacturer's protocol (Sigma-Aldrich) with own modifications. Previously prepared cell extracts were deproteinized with a 10 kDa MWCO spin Pierce Concentrator according to the manufacturer's protocol (Thermo Scientific). Deproteinized supernatants in a final volume of 50 μL were mixed with proper assay reagents supplied in the manufacturer's kit. The absorbance of samples, proportional to the amount of glucose-6-phosphate, was measured after 30 minutes of incubation at room temperature using a microplate reader Infinite 200 at λ = 450 nm. The value of the blank was subtracted each time. The amount of glucose-6-phosphate in the samples was determined from the standard curve and data were expressed as pmol per μL.

Pentose phosphate pathway enzyme activity assays

The total dehydrogenase activity (understood as the sum of both glucose-6-phosphate dehydrogenase (G6PD) and 6-phosphogluconate dehydrogenase (6-PGD) activities) and separately the 6-PGD activity were determined spectrophotometrically by measuring the rate of $NADP^+$ reduction at 340 nm according to [45] with our modifications. G6PD activity was calculated by subtracting the activity of 6-PGD from the total enzyme activity. To obtain the total dehydrogenase activity 0.2 mM NADP+, 0.4 mM D-glucose-6-phosphate, and 0.4 mM 6-phosphogluconate as reaction substrates were used. The substrates were added to 100 mM Tris-HCl buffer with pH 8.0 containing 1 mM $MgCl_2$. The addition of 5 μL cell extract (2 mg/mL) initiated the reaction. In turn, to obtain 6-PGD activity only 0.2 mM $NADP^+$ and 0.4 mM 6-phosphogluconate were used as reaction substrates. The kinetics of absorbance increase was recorded for 3 min using a microplate reader Infinite 200 at λ = 340 nm. The data were expressed in arbitrary units.

Determination of Mitochondrial Membrane Potential and Mitochondrial Network Morphology

Mitochondrial membrane potential (MMP) and mitochondrial network morphology were determined using rhodamine B hexyl ester. Cells from the exponential phase of growth were washed twice with sterile water and suspended in a 20 mM HEPES buffer with pH 7.4, containing 5% glucose. Incubation with 100 nM rhodamine B was conducted for 20 min in the dark at 28°C. After incubation, cells were harvested and resuspended in fresh HEPES buffer. The fluorescence was measured using a microplate reader Infinite 200 at λ_{ex} = 555 nm and λ_{em} = 579 nm. The mitochondrial network was also visualized using fluorescence microscopy at appropriate wavelengths. The microscopic images, which present typical results from the duplicate experiment, were captured with the Olympus BX-51 microscope equipped with the DP-72 digital camera and cellSens Dimension v1.0 software.

Determination of the Intracellular ATP Content

The level of ATP in yeast cells was determined with BacTiter-Glo™ Microbial Cell Viability Assay according to the manufacturer's protocol (Promega) with own modifications. Cells from the exponential phase of growth were suspended in a 100 mM phosphate buffer with pH 7.0, containing 0.1 % glucose and 1 mM EDTA. A sample of cell suspension with a density of 10^6 cells/mL was used for determination purposes. The luminescent signal, proportional to the amount of ATP, was recorded using a microplate reader Infinite 200, after the appropriate time (until the luminescence signal obtain a stable level). The data were expressed in arbitrary units. In addition, the level of ATP in yeast cells was determined after 30 min incubations of cells with different mitochondria respiration inhibitors (60 μM Antimycin A and 30 μM Oligomycin). The obtained data were expressed as a fold change in ATP content, after incubation with a particular inhibitor, in comparison to the level of ATP measured in yeast cells not exposed to inhibitors.

Biochemical measurements of ATP and ADP

The ATP and ADP levels were measured in whole cell extract according to [46] with own modifications. Cells from the exponential phase of growth (5×10^7 cells/mL) were harvested, washed with sterile water, and quickly resuspended in 90% acetone. The suspension was incubated at 90ºC for 15 min to evaporate acetone, with occasional high-speed vortexing. The remaining solution was centrifuged at 14 000 × g at 4°C for 7 min. The obtained supernatant was 10-folded diluted by its mixing with phosphate buffer (100 mM phosphate buffer; pH 7.0; 0.1 % glucose and 1 mM EDTA). The ATP and ADP levels in extracts were measured using ADP/ATP Ratio Assay Kit according to the manufacturer's instructions (Sigma-Aldrich). The principle of the assay involves the determination of ATP amount by measurements of D-

luciferin and luciferase-based luminescence. The amount of ADP is determined after its enzymatic conversion to ATP. Luminescence was recorded using a microplate reader Infinite 200, after the appropriate time (until the luminescence signal was stable). All samples were assayed at least three times and the value of the blank was subtracted each time. The results were presented as ATP, ADP, and the total ADP and ATP content. In addition, the ATP/ADP ratio was calculated.

Determination of ROS Content

The level of reactive oxygen species (ROS) was assessed with dihydroethidium (DHET; 10.7 μM final concentration; stock solution in DMSO). Yeast cells from the exponential phase of growth were washed twice with sterile water and suspended to a final density of 10^8 cells/mL in a 100 mM phosphate buffer with pH 7.0, containing 0.1% glucose and 1 mM EDTA. DHET was added to 200 μL of cell suspension and the fluorescence measurement was immediately performed. The kinetics of fluorescence increase due to oxidation of the fluorogenic probes, was measured immediately after the addition of the probe using a microplate reader Infinite 200 at 28°C at λ_{ex} = 518 nm, λ_{em} = 605 nm. ROS content was expressed as a relative rate of fluorescence increase.

In addition, the ROS content in yeast cells was determined after 30 min incubations of cells with different mitochondria respiration inhibitors (60 μM Antimycin A and 30 μM Oligomycin). The obtained data were expressed as a fold change in ROS content, after incubation with a particular inhibitor, in comparison to the level of ROS measured in yeast cells not exposed to inhibitors.

Determination of the cAMP Content

The level of cAMP in yeast cells was determined with Direct cAMP Elisa kit according to the manufacturer's protocol (Enzo Life Sciences) with its own modifications. Cells from the exponential phase of the culture (5×10^7 cells/mL) were centrifuged, washed with sterile water, and suspended in the YL buffer (1 M sorbitol, 0.1 M EDTA, 0.1% β-mercaptoethanol) containing lyticase (250 U per sample) for 30 min at 30°C. The resultant spheroplasts were lysed in a solution of 0.1 M HCl with 0.1% Triton X-100. Obtained extracts were centrifuged (12 000× g, 10 min, 4°C) to pellet cellular debris. Supernatants were transferred to fresh tubes and used for the determination of cAMP in acetylated format. 100 μL of acetylated samples were mixed with proper assay reagents supplied in the manufacturer's kit. The absorbance, inversely proportional to the amount of cAMP in samples, was measured using a microplate reader Infinite 200 at λ = 405 nm. The values of the blank and non-specific binding were

subtracted each time. The amount of cAMP in the samples was determined from the standard curve and data were expressed as pmol per mg of total protein.

Statistical analysis

The results are presented as mean ± SD from at least three independent experiments (apart from the determination of yeast reproductive potential). The statistical analysis was performed using the STATISTICA 13.3 software. The statistical significance of the differences between values obtained in a medium with glucose and fructose was evaluated using the t-test for independent samples. The statistical significance of the differences between yeast strains and cultivation conditions in comparison to WT strain culture in medium with glucose was evaluated using one-way ANOVA with the Tukey *posthoc* test. The homogeneity of variance was checked using Levene's test. The values were considered significant at $p < 0.05$. Used designation: differences between media with glucose and fructose * $p < 0.05$, ** $p < 0.01$, *** $p < 0.001$; differences in comparison to WT strain culture in a standard 2% glucose medium $^{\#}$ $p < 0.05$, $^{\#\#}$ $p < 0.01$, $^{\#\#\#}$ $p < 0.001$. The designation of other types of comparison is explained in the legend of the figure it concerns.

RESULTS

Fructose slightly increases the average reproductive potential of yeast cells, but significantly increases the maximum reproductive capacity

Nutrient availability is crucial for the production of energy and the biosynthesis of new macromolecules, including those needed for cell growth and proliferation. We previously reported that glucose concertation significantly modulates cell physiology and reproductive potential of the yeast cell [31, 32], but also that negative aspects of high glucose concentration (calorie excess) can be reduced by modulation of central carbon metabolism (CCM) and reduction of glucose uptake [30, 32].

To expand the links between CCM and the proliferative capacity of the cell, the question was asked whether, apart from the sugar concentration, the type of easily fermentable carbon source is also important. The analysis of the reproductive potential of yeast cells cultured in media with the same concentration of glucose or fructose was performed. Comparison between glucose and fructose medium was selected because both sugars are habitually identified as easily fermentable sources, but also some discrepancies between glucose and fructose utilization have been noted [36, 47]. Reproductive potential analysis showed that, in general, yeast cells grown on a fructose medium were able to produce more daughter cells compared to a glucose medium (Figure 1A). The difference in the reproductive potential of cells growing in glucose or fructose medium was modest (mean value 24.8 in glucose and 27.2 in fructose). Nevertheless, there were noticeable differences in the last section of the reproductive potential curves, relating to the maximum reproductive capacity of the cells (Figure 1A). On fructose medium, there was a group of cells that demonstrated increased reproductive potential, which was shown in violin plots presenting the differences in data distribution between analyzed culture conditions (Figure 1B) and in mean values of a maximum number of daughters determined for 10% of cells with the highest reproductive potential (Figure 1C). These results indicate that there are some differences between the fermentation metabolism of glucose and fructose, which influence long-term consequences in single-cell physiology and can modulate the reproductive potential of cells.

Fructose metabolism slightly decreases the growth rate, while slightly increasing the carrying capacity of the cell population

Carbon sources are used by cells in several cross-linking intracellular pathways. Although fructose fermentation is considered very similar to that of glucose, each change in CCM pathways may affect the physiological efficiency and vitality of the cell, which in turn can affect

the rate of cell population growth. There were apparent differences in the growth of the yeast cell population (Figure 2A-C). Yeast cells grown on fructose medium showed similar growth kinetics of the yeast cell population (Figure 2A) but slower growth rate compared to the yeast cells grown on glucose medium (Figure 2B). Nevertheless, the OD values at 24 and 36 h (corresponding to the carrying capacity) showed that yeast cells grown on fructose medium reach even higher cell densities than those grown on glucose medium (Figure 2C), consistent with increased maximum reproductive potential obtained for these cells (Figure 1A-C). These observations suggest that cell growth and reproductive potential of cells are interconnected.

The rate of carbohydrate utilization and activity of hexose transporters are lowered in the cells grown on fructose medium

Hexose uptake which can be carried out by several hexose transporters (Hxts) with different affinity is regarded as one of the critical steps in the metabolism of carbon sources during fermentation. To test how yeast cells adapt carbohydrate uptake and utilization not only to sugar concentration but also to the specific type of easily fermentative carbon sources, several parameters presenting the level and activity of Hxts in yeast cells grown on glucose or fructose medium were determined (Figure 3A-G). Considering that yeast cells possess several hexose transporters with different rate-affinity trade-offs [48, 49], the parameters for hexose transporters with outermost properties (Hxt1p – low-affinity and Hxt6p – high-affinity transporters) were tested. The level of the analyzed transporters was quantified by measuring the cellular Hxt-GFP fluorescence (Figure 3A, 3C), and their location was additionally checked by fluorescence microscopy (Figure 3B, 3D). Both parameters were tested in the cells from the exponential phase of growth, but also in cells cultured for a longer time (stationary phase and cells after 2 days), which is connected with the fact that Hxts are degraded in vacuole following endocytosis-mediated internalization [50, 51]. There were significant differences in the level and location of Hxt1p and Hxt6p in cells cultured on glucose and fructose medium (Figure 3A-D). The level of both transporters was lowered in cells grown on fructose medium, which was especially noted for an exponential phase of growth (Figure 3A, 3C). There were also clear differences in the location of Hxts between the analyzed culture conditions. In the exponential phase of the growth in glucose conditions, both Hxt1p and Hxt6p were located only in the cell plasma membrane. In contrast, under fructose conditions, Hxt1p, and Hxt6p were noted not only in the cell membrane but simultaneously inside the cell in the vacuolar space (Figure 3B, 3D). The observable differences between the glucose and fructose conditions were not the results of different (too high or too low) carbohydrate concentrations in the medium

(Supplementary Figure S1). In addition, the level of the analyzed Hxts decreased with the culture time, with a greater time-dependent decrease in the transporter level for Hxt6p, especially in the case of cells cultured on fructose medium (Figure 3A, 3C). As demonstrated by microscopic imaging, this decrease was due to the degradation of the transporter (Figure 3B, 3D). The expression level of *HXT1* and *HXT6* genes was calculated using the $-\Delta C_T$ method to compare yeast cells growing on glucose and fructose medium (Figure 3E–F). *HXT1* expression was shown to be down-regulated in cells grown in fructose medium. The expression level of the *HXT1* gene was approx. 50% lower in the fructose conditions than in glucose conditions (Figure 3E). For the *HXT6* gene, which encodes a high-affinity hexose transporter, an increased expression in the fructose conditions could be observed, although the changes in *HXT6* expression did not prove to be statistically significant (Figure 3F). As a result of the above changes, the observation of higher fructose concentration in comparison to glucose, noted in the medium at the analyzed point of cell culture time (Figure 3G), undoubtedly indicates that fructose (compared to glucose) is much slower taken up and used by yeast cells. This, in turn, may alter the metabolic pathways that determine the reproductive potential of the cells.

The activity of the pentose phosphate pathway and biosynthetic capabilities are reduced in the cells cultured on a fructose medium

Simple sugars are used intracellularly both as a substrate for energy generation and as a carbon skeleton for macromolecule biosynthesis. The PPP is a pathway in which carbohydrates can be used as a carbon source for biosynthesis and growing evidence indicates that cellular biosynthetic efficiency connected with cell size are important factor determining the reproductive potential of the cells [30, 32, 52-55]. Considering the above as well as differences in reproductive potential (Figure 1A–C), growth rate (Figure 2A–C), and the rate of carbohydrate uptake (Figure 3A–G), the analysis of parameters connected with the PPP and biosynthesis capacity for yeast cells grown on a medium with fructose were performed. It was noted that the level of Zwf1p (determined both by measuring GFP fluorescence and by microscopic imaging) was lower in the cells cultured on fructose medium compared to glucose medium (Figure 4A-B). In addition, the Zwf1p level decreased with the time of culture, although the difference in this level between cells grown in glucose and fructose mediums was alleviated (Supplementary Figure S2). However, *ZWF1* gene expression was slightly up-regulated in cells grown in a fructose medium (Figure 4C). The *e*xpression level of the *ZWF1* gene was approx. 30% higher compared to cells grown in glucose medium (Figure 4C). The content of G6P which is the main substrate for G6PD (glucose-6-phosphate dehydrogenase

encoded by *ZWF1*) was significantly higher in the yeast cells grown in fructose medium compared to glucose medium (Figure 4D). Moreover, analysis of the PPP enzyme activity (G6PD and 6-PGD) showed that this pathway was less active in the cells grown in the medium with fructose. Cells growing in fructose medium showed lower activity of both G6PD and 6-PGD enzymes, which results in significantly lower total PPP dehydrogenases activity (Figure 4E). Since PPP is directly related to the level of biosynthesis, and proteins usually make up just over half of the cell content, the observation of lower protein content per cell in the fructose medium (Figure 4F), clearly demonstrates that in the fructose medium (compared to glucose) cell display lower biosynthetic capacity. This further confirms that there is a close relationship between metabolic pathways, cell biosynthetic efficiency, size, and reproductive capacity.

Fructose-depended metabolic flux increased mitochondrial activity and ATP production without higher ROS generation

The physiological efficiency of the cell results from a metabolic trade-off between different ways of carbohydrate utilization [5, 6, 30]. In yeast, the cAMP/PKA pathway is a major glucose-signaling pathway that adjusts cell metabolism to the nutrient status. When glucose is available, activation of the cAMP/PKA pathway stimulates glycolytic flux, inhibits respiratory metabolism gene expression, induces ribosome biogenesis, and inhibits the stress response. We previously reported that glucose concentration (calorie restriction and calorie excess conditions) can noticeably modulate the activity of the cAMP/PKA pathway and that reduced activity of the cAMP/PKA pathway under CR conditions may increase the reproductive potential of the yeast cell [32]. Considering the above and observations noted for cells cultured in fructose medium, we tested how fructose modulates the energy metabolism of the cells (Figure 5A-I). The mitochondrial membrane potential (MMP) and mitochondrial network morphology analyzed with rhodamine B (Figure 5A, B) showed that although cells grown in fructose and glucose use fermentative metabolism, this is not an unambiguous arrangement, and cells using fructose have increased metabolism redirection toward respiratory activity than cells growing on glucose. The MMP was significantly higher (Figure 5A) and the mitochondrial network was more developed (Figure 5B) in cells growing on a fructose medium compared to cells growing on glucose. To further confirm these unpredictable differences in mitochondrial activity, changes in intracellular ATP, ADP content, and ATP/ADP ratio in cells growing in glucose or fructose medium were examined (Figure 5C-G). The level of ATP was checked both in the living yeast cells (Figure 5C) and also in whole cell extract (Figure 5D). Regardless of the type of measurement used, the ATP content was higher (approximately 20-30%) in the case

of cells cultured in the fructose medium in comparison to cells cultured in the glucose medium (Figure 5C, D). The level of ADP was similar in both analyzed growth conditions (Figure 5E), but the ADP+ATP pool was significantly higher in cells grown in the fructose medium (Figure 5F), which indicates that the higher level of ATP noted under these conditions was not the results of a simple conversion of ADP to ATP and the level of ADP must be maintained. In addition, the ATP/ADP ratio, which has recently been considered an important regulator controlling the transition between aerobic glycolysis and oxidative phosphorylation [56, 57], was almost 50% higher in the case of cells cultured in the fructose medium compared to cells cultured in glucose medium (Figure 5G). Since the cAMP/PKA pathway adjusts cell metabolism to the nutrient status and its increased activity stimulates glycolytic flux, the observation of lower cAMP content in the cells growing in fructose medium (Figure 5I), additionally confirms that fructose metabolism is connected with increased metabolism redirection toward respiratory activity. Moreover, the level of ROS estimated with DHET, showed that redirection toward higher respiratory activity on the fructose medium was not associated with an increased ROS generation. The ROS content in cells growing in a fructose medium was even lower than the ROS content noted for the glucose medium (Figure 5H). The presented results prove that fructose and glucose involve particular intracellular metabolic pathways to a different extent, which modulate the energetic and biosynthetic capability of the cells influencing their reproductive potential. Moreover, the results imply that redirecting of the carbon/metabolic flux and adjustment in the activity of the cAMP/PKA pathway plays a critical role in response to changes in nutrient availability. Thus the presented results are another confirmation of our previously postulated conception of links between CCM changes and the proliferative capacity of the cells [33].

Fructose-depended metabolic flux toward increased respiratory activity is confirmed by data obtained with cells devoid of hexokinase 2

It is generally known that hexokinase isoenzyme 2 − Hxk2p plays a key role in the intracellular glucose-signaling pathway. Several data show that the Δ*hxk2* mutant strain exhibits increased respiratory activity [30, 58, 59], although our previously reported results [30] suggest that besides increasing respiration, deletion of the *HXK2* gene results in redirection in the glucose-utilization pathway. To extend the insights and further confirm the metabolic features noted for cells growing in a fructose medium, a comprehensive analysis was performed using cells of Δ*hxk2* strain growing under conditions with glucose and fructose. The MMP of the Δ*hxk2* strain was already significantly higher in comparison to cells of the WT strain, in the case of cells

cultured in a glucose medium. However, culturing cells of Δ*hxk2* strain in the medium with fructose further noticeably increases MMP (Figure 6A). Similarly, the mitochondrial network was generally more developed in Δ*hxk2* cells compared to the WT strain, and the most developed mitochondrial network was observed for Δ*hxk2* cells growing in a fructose medium (Figure 6B). As a result of higher mitochondrial activity, the ATP level was higher in the Δ*hxk2* strain tested both in the live yeast cells (Figure 6C) and also in whole cell extract (Figure 6D). Regardless of the type measurement used, the ATP content in the Δ*hxk2* strain cultured in the glucose medium was about 50-70% higher compared to the WT strain. Moreover, culturing cells of the Δ*hxk2* strain in the fructose medium further increased the level of ATP (about 60 % compared to Δ*hxk2* cells cultured in glucose medium, and 2.5 times more compared to WT cells cultured in glucose medium) (Figure 6C, D). The level of ADP was almost identical both in the analyzed growth conditions and between WT and Δ*hxk2* strains (Figure 6E), but the ADP+ATP pool was significantly higher in the Δ*hxk2* strain compared to the WT strain, especially in cells of the Δ*hxk2* strain cultured in the medium with fructose (Figure 6F). What is more, particularly large differences between the WT and Δ*hxk2* strains were noted in the ATP/ADP ratio values (Figure 6G). The ATP/ADP ratio was 2 times higher for the Δ*hxk2* strain cultured in the glucose medium and 3 times higher for the Δ*hxk2* strain cultured in the fructose medium compared to the WT strain cultured in the glucose medium (Figure 6G). In addition, there were also changes in the content of cAMP in cells of the Δ*hxk2* strain (Figure 6I). The content of cAMP was about 40% lower in cells of the Δ*hxk2* strain cultured in the glucose medium compared to the WT strain cultured in a glucose medium, and even lower in a medium with fructose (Figure 6I). Consistent with the previously noted trend (Figure 5H), the observed higher respiratory activity does not seem to be associated with an increased ROS generation. In general, the ROS content for the Δ*hxk2* strain was lowered compared to the WT strain (Figure 6H). The presented results confirm that the Δ*hxk2* strain exhibits increased respiratory activity, but more importantly, they further strengthen the evidence that fructose metabolism redirects carbon flux toward higher mitochondrial activity, which is also associated with a decrease in the activity of the cAMP/PKA pathway.

The changes in ATP level and ROS content under conditions impairing mitochondrial activity are more pronounced for yeast cells cultured in a fructose medium

Mitochondria have multiple sites from which ROS can be generated and according to this, the free radical theory of aging indicates their unequivocal responsibility for cell damage [60]. However, the concept of respiratory activity and mitochondria as the main source of ROS is

now increasingly questioned. Both the important signaling functions of ROS and the possibility of their generation from non-mitochondrial sources are emphasized [30, 31, 61, 62]. Given this, and the observation that redirection toward higher respiratory activity was not associated with an increased ROS generation (even lower ROS content was noted) (Figure 5H,6H) the analysis of changes in ATP level and ROS content in conditions mimicking respiratory failure were performed (Figure 7A, B). To impair mitochondrial activity cells were treated with mitochondrial respiratory inhibitors: antimycin A, a respiratory-chain complex III inhibitor, and oligomycin, a blocker of proton translocation through ATP-synthase. It was noted that both inhibitors significantly reduced ATP content and increased ROS content compared to the output values, regardless of the yeast strain used (Figure 7A, B). However, it can be observed that the fold-change in values of ATP and ROS content increased with conditions that determine increased mitochondrial activity. Yeast cells cultured in a fructose medium have a higher decline in ATP and a higher rise in ROS content compared to cells cultured in a glucose medium, regardless of the strain used. The largest decrease in the ATP content and simultaneously the largest increase in the ROS content was noted for cells of the Δ*hxk2* strain growing in a fructose medium (Figure 7A, B). The presented results confirm that fructose metabolism is associated with increased respiratory activity compared to glucose metabolism, but more importantly, they showed that under physiological conditions, an increase in mitochondrial activity is not necessarily associated with increased ROS generation. Nevertheless, mitochondria as a source of intracellular ROS may play a dominant role in respiratory failure conditions.

The decreased activity of PPP, reduced biosynthetic capabilities and reduced rate of carbohydrate utilization are confirmed in cells devoid of hexokinase 2

Since the energy metabolism of yeast cells seems to be adapted to the presence of fructose or glucose in the medium, several parameters related to the rate of carbohydrate uptake (Figure 8A–D) and parameters connected with the PPP and biosynthesis capacity (Figure 8E–H) were determined also in cells of the Δ*hxk2* strain. First of all, the level of hexose/glucose uptake measured with the fluorescent non-hydrolyzable glucose analog 6-NBDG was significantly reduced in the Δ*hxk2* strain compared to the WT strain (Figure 8A). The expression level of *HXT1* and *HXT6* genes differ between WT and Δ*hxk2* strains (Figure 8B, C). *HXT1* gene expression was down-regulated, whereas *HXT6* gene expression was up-regulated in the Δ*hxk2* strain (Figure 8B, C). The *HXT1* gene expression level was approx. 3 times lower for Δ*hxk2* cells (in both glucose and fructose conditions) compared to WT cells cultured in glucose

medium. The *HXT6* gene expression level was approx. 4 and 6 times higher for Δ*hxk2* cells cultured in glucose or fructose medium in comparison to WT cells cultured in a glucose medium (Figure 8B, C). In addition, cells of the Δ*hxk2* strain in comparison to the WT strain showed a significantly slower rate of carbohydrate utilization (Figure 8D). Also in the case of the Δ*hxk2* strain, the rate of fructose utilization was lower than glucose utilization, although this was dependent on the cultivation time and the differences were generally smaller (Figure 8D).

The analysis of the PPP-related parameters showed that, in general, the activity of this pathway and connected with its biosynthesis capacities were reduced for cells of the Δ*hxk2* strain (Figure 8E-H). G6P content was significantly higher in the Δ*hxk2* strain, although there was no further increase in G6P level between the Δ*hxk2* strain cells cultured in fructose medium compared to the glucose medium (Figure 8E). The activity of the PPP enzymes (G6PD and 6-PGD) was lower in the Δ*hxk2* strain compared to the WT strain cultured in a glucose medium (Figure 8F). The activity of G6PD and 6-PGD was not different between cells of the Δ*hxk2* strain cultured in fructose medium and glucose medium (Figure 8F). *ZWF1* gene expression was up-regulated in the Δ*hxk2* strain (Figure 8G). Cells of the Δ*hxk2* strain growing in fructose medium and glucose medium had a comparable level of *ZWF1* gene expression. The expression level of the *ZWF1* gene was approx. 1.5 times higher for Δ*hxk2* cells compared to WT cells cultured in glucose medium (Figure 8G). The PPP enzymes activities and the significantly lower protein content per cell noted in the cells of Δ*hxk2* strain cultured both on fructose and glucose medium (Figure 8H), show that the metabolic flux toward increased respiratory activity is associated with decreased biosynthetic capabilities of the cells. The results also showed that *HXK2* deletion or fructose metabolism alters the metabolic flux in carbon metabolism pathways, where only one of the effects is increased respiration.

The metabolic flux toward increased respiratory activity reduces the growth rate

Since the metabolic flux toward increased respiratory activity was found to reduce biosynthetic capabilities, we further analyzed the rate of cell population growth using the Δ*hxk2* strain. There were differences in the growth of the yeast cell population (Figure 9A-C). The cells of the Δ*hxk2* strain showed different growth kinetics of the yeast cell population (Figure 9A) and significantly lower growth rate compared to the cells of the WT strain growing in glucose medium (Figure 9B). Nevertheless, the OD values after 24 and 36 h showed that, despite the slower growth rate, the cells of the Δ*hxk2* strain reached a cell density comparable to the WT strain on glucose medium (Figure 9C). The results also confirm that the maximum number of

cells in the population is slightly higher in a fructose medium than in a glucose medium (Figure 9C).

Fructose-depended metabolic flux toward increased respiratory activity and lower biosynthetic capabilities affects the reproductive potential of yeast cells

To further investigate the relationship between central carbon metabolism, respiratory activity, cell biosynthetic efficiency, and cell proliferative capacity, analyses of reproductive potential in Δ*hxk2* mutant under conditions with glucose or fructose were performed. Analysis of the reproductive potential showed, that in general, cells of the Δ*hxk2* strain, regardless of the growth conditions, were able to produce more daughter cells compared to the WT strain (Figure 10A). Although the difference in overall reproductive potential between cells of the Δ*hxk2* strain cultured in glucose or fructose medium was not statistically significant (mean value 32.0 on glucose and 33.9 on fructose medium), some slight differences related to the maximum reproductive capacity of the cells can be noted (Figure 10A). There was a group of cells showing an increased reproductive potential, as demonstrated in the violin plots (Figure 10B) and by values of a maximum reproductive potential (Figure 10C). However, it is worth noting that changes in reproductive potential between cells cultured in conditions with glucose or fructose are more pronounced for the WT strain compared to the Δ*hxk2* strain (Figure 10A-C). These results confirm that there are metabolic differences between the cellular utilization of glucose and fructose, that have long-term consequences in single-cell physiology and modulate their reproductive potential.

DISCUSSION

Carbohydrate plays a critical role in cellular metabolism, thus their utilization must be tightly controlled and adjusted to changes in extracellular conditions and intracellular demands. Analyzing carbohydrate metabolism and its influence on the organism's and cell physiology seems to be more and more important due to a diet rich in simple carbohydrates and the global healthcare epidemic of obesity, type 2 diabetes, cardiovascular diseases, and metabolic syndrome [63-65]. The calorie excess is associated primarily with a high supply of glucose, but it can also be considered in the case of other simple sugars, such as fructose. The molecular aspects of fructose metabolism and its excessive consumption resulting from the increased share of sucrose and high-fructose corn syrup (HFCS) in the diet have been underlined as an important factor leading to multiple human metabolic diseases [66, 67], but also as a factor involved in neurotoxicity and decreased organism healthspan [68]. Although, several reports indicate the role of excessive fructose consumption in the development of metabolic diseases, the impact of fructose metabolism at the cellular level is not yet well understood. The aspect of fructose metabolism is just as little known in the case of yeast cells. Most of the known studies using yeast analyzed discrepancies between glucose and fructose fermentation in the context of industrial bioprocesses and wine fermentation when a high residual fructose level at the latter stages of fermentation is undesirable and can lead to stuck or sluggish fermentation [34-36, 47]. Currently, there are only limited data concerning the cellular mechanism of fructose impact in the case of yeast [37, 38] and there are almost no studies analyzing fructose metabolism in the context of the reproductive potential (replicative lifespan) of yeast cells. The only known to authors studies analyzing the impact of carbohydrate composition of media, including fructose, on replicative lifespan concern lager yeast (*Saccharomyces pastorianus*) [69]. The experimental approach used in this work provides comprehensive explanations of the differences between intracellular glucose and fructose metabolism, which may be useful both in the context of industrial fermentation and in understanding the health aspects of consuming carbohydrates.

The fructose metabolism and reproductive potential of the cells

The data presented here provide new information supporting that there exist discrepancies between glucose and fructose energy metabolism [33-36, 47]. What is new, they additionally show how cellular metabolism is altered by fructose and what long-term consequences it may have on cellular physiology and their ability to proliferate. In the case of yeast cells, the ability to reproduce (referred to as replicative lifespan or reproductive potential) is expressed by the number of daughter cells produced by the mother cell during her lifetime [29, 41]. The

reproductive potential of yeast cells can be significantly modulated by changes in nutrient content, thus it can be observed both substantial increases (e.g. in the caloric restriction condition) [29, 70], as well as decreases (e.g. in the conditions of glucose excess) [30, 32] values of this parameter. Hence, to answer the question of whether two easily fermentable carbon sources glucose and fructose may have different impacts on the reproductive capacity of the yeast cells, we performed a comprehensive analysis of several cellular parameters. Our findings present that fructose in comparison to glucose slightly increases the reproductive potential of the cells (Figure 1A-C). The observable changes can be overlooked from the ecological point of view, where high competitive abilities [7, 10] are dependent mainly on the youngest cells which performed only a few generations. Despite minor differences in the mean value of the reproductive potential of the cells (Figure 1A), fructose has a significant impact on the maximal value of this parameter (Figure 1B-1C) which is very important for maintaining the physiological efficiency of cells as long as possible. The wide range of performed analyses allowed us to identify several interrelated aspects of cellular metabolism, altered by the presence of fructose. They include: (i) changes in hexose transporters activity and lower carbohydrate uptake (Figure 3); (ii) changes in carbon catabolite repression and lower activity of cAMP/PKA pathway which trigger increased metabolism redirection toward respiratory activity (Figure 5); (iii) changes in PPP activity and decrease the biosynthetic capabilities of the cells (Figure 4 and Figure 2). All of the observable metabolic changes caused by the presence of fructose were supported by the results obtained in the experimental approach using Δ*hxk2* strain which is known for disrupted glucose repression and exhibition of increased respiratory activity (Figures 6-10). Moreover, the presented data shed somewhat new light on the role of mitochondria and respiratory activity in the generation of ROS, which seems to be dual and differ between physiological and respiratory failure conditions (Figures 5H; 6H; 7).

Hexose transporters activity and carbohydrate uptake

Although glucose and fructose are easily fermented carbon sources, several works present preferential use of glucose over fructose in the case of yeast cells [33-36, 47]. The precise molecular mechanism and cause of this preferential utilization are not fully understood, but the discrepancy in glucose/fructose fermentation seems to be connected with the differential transport rate of those sugars across the plasma membrane and hexose transporters affinities [33-35] and/or differences in hexokinase kinetic properties and rate of hexose phosphorylation inside the cell [34, 35, 47].

The results of hexose transporters' activity and carbohydrate uptake (Figure 3 and Figure 8A-D) obtained in this work confirm the role of hexokinase and hexose transporters in fructose metabolism. The rate of fructose uptake was significantly lower in comparison to the rate of glucose uptake and this rate was even lower in the case of Δ*hxk2* (Figure 3G and 8D). This is in line with data on sugar utilization noted previously [34, 35, 47] and also with the observation that deletion of *HXK2* decreases the rate of glucose uptake (Fig. 8A); [31]. The transport of glucose and fructose can be carried out by several joint Hxt proteins with different hexose affinity [48, 49]. It was noted that lower uptake of fructose in comparison to glucose is mainly the result of significantly lower expression of the *HXT1* gene and lower level of Hxt1p noted in those conditions (Figures 3A-B; 3E). The effect of *HXT1* gene expression on the rate of carbohydrate uptake was also confirmed using Δ*hxk2* strain (Figure 8D). The observable crucial role of Hxt1p in sugar uptake can be explained by the rate-affinity trade-off, which assumes that a higher rate of carbohydrate transport is connected with a lower affinity for this carbohydrate and those criteria are fulfilled by low-affinity transporters such as Hxt1p and Hxt3p [49]. The leading role of low-affinity hexose transporters in carbohydrate uptake capacity seems to be also confirmed by several studies where the level of those transporters was associated with glucose utilization ratio, glycolytic flux, and cell cycle progression [33, 71-73]. Moreover, literature data showed that the activity of low-affinity transporters and connected with it higher glucose uptake rate correlates with a higher growth rate [72, 74]. This is also noted in this work, where lower levels and expression of the *HXT1* gene (Figures 3A-B; 3E; 8B) correlate with a reduced growth rate (Figures 2 and 9). The results of *HXT1* gene expression noted in Δ*hxk2* strain also confirm the existence of interplay between hexokinases presence (especially hexokinase 2) and hexose transporters activity which was recently noted both in *S. cerevisiae* [74] and *Yarrowia lipolytica* [34] yeast cells. The connection between fructose metabolism, hexokinase, and hexose transporters is additionally supported by the results of the level and expression of high-affinity transporter *HXT6* (Figures 3C-D; 3F; 8C). *HXT* genes are generally co-expressed [49] and high-affinity transporters Hxt6p and Hxt7p can be noted even when relatively high sugar concentrations are still present [73]. However, it is well known, that expression of high-affinity and moderate to high-affinity (*HXT2* and *HXT4*) transporters are induced when the glucose level is falling and cells gradually move to the stationary phase [73], but also their expression is inhibited by glucose catabolite repression mediated by Hxk2p [74]. This suggests that cells growing on fructose in comparison to glucose may have both lower intracellular levels of carbohydrates (due to lower sugar uptake rate) but also receive a different nutrient signal which is read as lower than actual sugar concentration (mimicking nutrient-

scarce signal). The obtained results show that fructose-mediated catabolite repression is lowered compared to glucose repression. Reduced catabolite repression in the case of fructose metabolism can be indicated by the results of increased expression of high-affinity transporters (Figure 8C), but also by the results showing downregulation of *HXK2* and upregulation of *HXK1* gene in cells cultured in fructose medium (data not shown). Alongside, it is worth underlining the results of the level and the location of analyzed transporters (Figure 3A-D) which shows that Hxts can be also controlled at post-transcriptional (lower level of Hxt6p on fructose medium despite its higher expression) and post-translational level (different intracellular location of GFP-Hxts signal and differences in transporter degradation between glucose and fructose conditions).

The catabolite repression and metabolism redirection toward respiratory activity by reducing the activity of the cAMP/PKA pathway

Due to observable differences and literature analysis, we assumed that fructose metabolism in comparison to glucose decreased the activity of the cAMP/PKA pathway. The obtained results concerning parameters related to mitochondrial function and metabolism (Figure 5) support this assumption and clearly state that fructose metabolism results in an increased redirection of metabolism towards respiratory activity (Figure 6). Firstly, fructose metabolism resulted in lowered cAMP content (Figures 5I and 6I) suggesting that the intracellular signal originating from fructose conversion is different compared to glucose conversion. This high-probably modifies the glycolytic-dependent intracellular route of cAMP/PKA activation based on RAS, which is in line with previously presented data showing that: (i) high glycolytic flux connected with Hxk2p-dependent glucose repression and intracellular sugar phosphorylation is necessary for activation of the cAMP/PKA pathway [58, 75]; (ii) fructose-1,6-bisphosphate (F1,6bP) function as an activator of RAS and deletion of *HXK2* gene abolishes glucose-induced activation of RAS [26]; (iii) cAMP peak and response are lower in the case of cell transitioned from nonfermentable carbon sources to fructose with comparison to cell transitioned to glucose [76]; (iv) cAMP/PKA pathway negatively regulates endocytosis of Hxt1p [77]. What is more, both the cAMP signalling pathway and carbohydrate uptake with glycolytic flux play important roles in cell proliferation [71, 78, 79]. It was previously shown that activation of the cAMP/PKA pathway and high metabolic flux increases the level of cyclin Cln3 [71, 78] and that impaired fermentation, caused among others by the loss of *HXK2*, decreased but not blocked the expression of *CLN3* and *CDC28* genes [79]. Furthermore, the reproductive potential observed both under fructose conditions (Figures 1 and 10) and in the case of the Δ*hxk2* strain ([30]; this

work) together with reproductive potential determined in Δ*gpa2* and Δ*grp1* strains [32] and others yeast mutants and circumstances [80] point out to a significant role of the cAMP/PKA pathway in the proliferative capacity of the cell. Therefore, actions leading to a reduction the activity of the cAMP/PKA pathway seem to extend the reproductive potential of the yeast cells ([30, 32]; this study).

The fructose metabolism results in decreased activity of the RAS/cAMP/PKA pathway, and lowered the catabolite repression, the consequence of which is the modification of the transition between aerobic glycolysis and oxidative phosphorylation. The results concerning mitochondrial function and metabolism obtained in this work (Figure 5), clearly demonstrate that fructose metabolism is connected with increased metabolism redirection toward respiratory activity and such unanticipated conclusions were further confirmed by using Δ*hxk2* strain (Figure 6) and conditions impairing mitochondrial activity (Figure 7). Higher mitochondrial activity and increased levels of ATP production noted for cells growing in fructose medium and also in the case of Δ*hxk2* strain can be explained by several features connected with (i) differences in the metabolic trade-off between glucose and fructose utilization pathways; (ii) ability to regulate metabolic pathways through the produced metabolites, especially the glycolytic metabolites; (iii) lower usage of ATP.

Firstly lower activity of the RAS/cAMP/PKA pathway and impaired catabolite repression noted in the case of cells growing in a fructose medium released the expression of several respiratory metabolism genes, which stay in line with data concerning the relationship between cAMP/PKA signaling, glycolysis and respiratory activity [25, 26, 81]. Then, yeast cells growing even under relatively high levels of carbohydrates conduct a metabolism which is a mix of fermentation and respiration, and both processes can run in parallel to support the metabolic needs of the cells. Such possibility was noted i.e. in research presenting a metabolic model concerning the switch between respiration and fermentation in yeast [82], by data showing the metabolic intermediates benefits supplied by respiratory activity in the context of proliferation of yeast cells during fermentation [16, 17]. Other important factors controlling metabolic flux are the glycolytic intermediates, especially fructose 1,6-bisphosphate (F1,6bP) and glucose-6-phosphate (G6P) [15, 26, 83, 84]. F1,6bP inhibits the activity of respiratory chain complex II and III, although its level also indicates the glycolytic flux and correlates with the glucose uptake rate [15, 83, 84]. G6P is regarded as a stimulator of the respiratory chain, and its level is connected with the regulation of respiration [84]. Hence, higher mitochondrial activity and increased levels of ATP production were noted for cells growing in a fructose medium, and in the case of Δ*hxk2* strain can be also caused by changes in the level of G6P and

F1,6bP. Such possibility seems to be confirmed both by the results of a higher level of G6P observed in the case of fructose metabolism (Figure 4D) and Δ*hxk2* strain (Figure 8E; [30]) and the low level of F1,6bP observed in Δ*hxk2* strain [84, 85]. Further, an extremely important but somewhat overlooked role in controlling the transition between mitochondrial metabolism and aerobic glycolysis is played by the ATP/ADP ratio [57]. The work of Maldonado and Lemasters underlines that a high cytosolic ATP/ADP ratio generated by aerobic mitochondrial metabolism suppresses glycolysis and conversely, a lower ATP/ADP ratio is necessary to maintain the increased glycolysis characteristic for highly proliferating cells. Our previous studies and results obtained in this work seem to perfectly confirm this assumption, because a high ATP/ADP ratio was accompanied by increased mitochondrial activity and, at the same time, by a lower rate of cell growth and proliferation (Figures 2; 5; 6; 9). Moreover, our results obtained using Δ*hxk2* strain together with literature data presenting voltage-dependent anion channel (VDAC) role in mitochondrial metabolism [57] and mitochondria-related noncanonical functions of hexokinases [86] support clarification of this aspect. Respiratory substrates and other polar metabolites pass the outer mitochondrial membrane through VDAC and relative closure of VDAC limits oxidative phosphorylation and decreases ATP/ADP ratio [57]. An important role in the regulation of VDAC permeability plays mitochondrial-bound hexokinase 2 and free tubulin which are distinctive for highly proliferating cells. The ATP is exported from mitochondria by VDACs, thus Hxk2p binds to VDAC to maximize the ATP-using phosphorylation reaction. The connection between VDAC and hexokinases can be severed by high G6P concentrations which among other results in glycolysis inhibition [86]. Therefore, we assumed that lack of Hxk2p (Δ*hxk2* strain) or its lower level (fructose conditions) on one hand released the expression of respiratory metabolism genes, but on the other allowed VDAC opening resulting in easier penetration of substrates into the mitochondria and also in reduced direct hexokinase-depended usage of ATP. The lower usage of ATP in the case of Δ*hxk2* strain and cells growing in fructose medium can be additionally explained by the lower activity of the cAMP/PKA pathway (lower usage of ATP for cAMP synthesis) and lower biosynthetic capabilities (Figures 2; 4; 8; 9) because about half of the energy generated in CCM is used for macromolecular synthesis, especially for protein synthesis [15].

Changes in PPP activity and reduction in the biosynthetic capabilities of the cells

The connection between energy-producing and biomass formation pathways is generally closed in the metabolic triangle – the respiration-glycolysis-pentose phosphate pathway [30]. An important role in this relationship play the glucose uptake rate and glycolytic flux, which

form the one hand favor fermentation and production of building blocks, but on the other hand, reduce respiration capabilities. Hence, it can be observed phenomenon that ATP is produced by respiration when the glucose uptake rate is low [30, 31, 74, 83, 87] and such an assumption is also consistent with observations of this study. Nonetheless, a high carbohydrate uptake rate and high glycolytic flux will correspond to decreased respiratory metabolism, but also to a higher biosynthetic rate. An important role in cellular biosynthesis plays PPP providing intermediates necessary for the production of macromolecular components [88]. There can be observed inversed correlation between results concerning PPP activity, overall biosynthetic capabilities of cells (Figures 4; 8E-H), and results concerning mitochondrial function and metabolism (Figures 5; 6). Cells growing in the fructose medium and cells of Δ*hxk2* strain exhibit lower carbohydrate uptake rate, lower fermentation yield [31], increased respiration metabolism, and a higher level of ATP but also lower activity of PPP, decreased biosynthetic capabilities, and decreased growth rate. The level and activity of Zwf1p decreased in cells cultured in a fructose medium although the expression of its gene increased (Figures 4A-E; 8E-G). The explanation of this phenomenon may be connected with post-transcriptional and post-translational levels of control, but also with transcriptional changes caused by metabolic modification. Previously published data showed that expression of *ZWF1/G6PD* can be regulated by the NADPH/NADP ratio, but also by cAMP-dependent inhibition of *ZWF1* transcription [89].

The importance of metabolic changes in the context of respiratory activity and cellular biosynthetic possibilities has a crucial impact on the reproductive potential of the cell. This work and our previous findings [30, 32] demonstrate that alterations increasing respiratory activity, but what is important simultaneously decreasing the overall biosynthetic capabilities, increase reproductive potential of the cell (Figures 1;10). The connection between biosynthetic capabilities, especially protein biosynthesis, and the disturbance in proliferation or decline in reproductive potential was also noted in other studies [30, 32, 90, 91]. The obtained results confirm also the positive impact of low glycolytic flux and decreased PKA activity on cell reproductive potential [32, 92, 93]. Furthermore, the increased maximal reproductive potential observed in the case of cells growing in the fructose medium is another data showing that redirection towards increased respiration activity is connected with extending yeast lifespan. Such a mechanism has been postulated for a long time, especially to explain the action of calorie restriction (CR) on yeast lifespan [30, 59, 94-96]. We consider, however, that this is highly probable that the increased reproductive potential noted in the case of Δ*hxk2* strain and under fructose or CR conditions (this work; [30]), is not a direct result of increased respiratory

metabolism but a consequence of overall changes in metabolic fluxes. Such assumption is in line with data postulated that chronological lifespan (CLS) is determined by remodeling cell metabolism from fermentation to respiration [97] and would also explain the challenging issue of the extended replicative lifespan in respiratory-deficient yeast cells (rho^0) [98, 99].

The fructose metabolism and RFT generation

The results obtained in this work also shed somewhat new light on the intracellular generation of ROS. The concept of mitochondrial respiration as the major cellular source of ROS and the exclusively damaging role of ROS has been challenged over the last few years. There are growing number of evidence suggesting signalling role of ROS [100, 101] but also more and more studies underline the existence of non-mitochondrial ROS sources within the cell [30, 31, 62, 102, 103]. The results presented here further point out that the relationship between the type of metabolism, sources of ROS generation, its cellular role, and lifespan is more complex. Our data suggest that (i) non-mitochondrial sources can be an important pool of ROS in yeast cells, especially under fermentative metabolism, which confirmed previously noted dependencies [30, 31, 93, 102]; (ii) enhancement of oxidative metabolism and mitochondrial activity by the hormesis effect and sealing the respiratory chain may prevent uncontrolled proton leakage, and thus reduces ROS generation, what was also recently postulated [31, 94, 97, 104]; (iii) significantly increased level of ROS is noted in conditions impairing mitochondrial activity, what was also shown by other works [81, 105]. Moreover, data recently published by Mori et al. shows a new intriguing possibility by which higher respiratory activity and increased development of the mitochondrial network may reduce ROS generation. The authors demonstrate that mitochondrial respiration reduces intracellular availability of oxygen and respiring mitochondria that surround the nucleus decrease nuclear exposure to oxygen [106].

In summary, we report here that the discrepancies between the fermentation of glucose and fructose are caused by changes in interrelated intracellular metabolic pathways. This could have long-term implications, as those relating to the reproductive potential of cells. These fructose-derived changes in CCM resulting in lower glycolytic flux, increased redirection toward respiratory activity, and lower overall biosynthetic capabilities seem to be the reason for higher reproductive potential noted for cells growing in fructose medium. This explanation, additionally supported by results obtained for Δ*hxk2* strain, suggests why increased respiration is important, but is not a sufficient condition for a reproductive potential extension. Moreover, this study suggests that redirection in carbohydrate-utilization pathways and metabolic adaptations have a relevant impact on the proliferative capacity of cells.

Acknowledgments

We are grateful to Associate Prof. Adrianna Skoneczna and Prof. Maya Schuldiner for providing the HXT1-GFP yeast strain originating from yeast GFP clone collection (Huh et al., 2003).

This research was funded in whole by the Polish National Science Centre (Grant No.: 2021/05/X/NZ3/00162). For the purpose of Open Access, the author has applied a CC-BY public copyright licence to any Author Accepted Manuscript (AAM) version arising from this submission.

Author contributions

Roman Maslanka: Conceptualization; methodology; investigation; visualization; formal analysis; project administration; data curation; writing–original draft; writing–review and editing; supervision; funding acquisition. **Sabina Bednarska**: Methodology; investigation; formal analysis. **Renata Zadrag-Tecza:** Conceptualization; methodology; investigation; formal analysis; writing–original draft; writing–review and editing.

Conflict of interest

The authors declare that they have no conflict of interest.

FIGURE LEGENDS

Figure 1. ***The reproductive potential of WT yeast cells cultured in glucose or fructose medium with glucose or fructose*** (**A**) The reproductive potential of yeast cells growing in glucose or fructose conditions, (**B**) Distribution of reproductive potential in population of yeast cell growing in glucose or fructose conditions, (**C**) Maximal reproductive potential determined on the basis of 10% yeast cells with the highest number of daughters cells. The data represent the mean values from two independent experiments of 40 cells each. * $p < 0.05$; *** $p < 0.001$ as compared between media with glucose and fructose.

Figure 2. ***The growth of WT yeast cell population cultured in medium with glucose or fructose*** (**A**) Growth kinetic of yeast cell population monitored during 12 h, (**B**) The growth rate of yeast cell population, (**C**) The growth of the yeast cell population monitored after 24 h and 36 h. The results are presented as mean ± SD from three independent experiments. * $p < 0.05$; ** $p < 0.01$ as compared between media with glucose and fructose.

Figure 3. ***The hexose transporters activity and carbohydrate uptake in WT yeast cells cultured in medium with glucose or fructose*** (**A**) Relative low-affinity hexose transporter level quantified by Hxt1-GFP fluorescence measurements after different time of cell cultivation, (**B**) Intracellular location of Hxt1-GFP signal determined by fluorescence microscopy after different time of cell cultivation, (**C**) Relative high-affinity hexose transporter level quantified by Hxt6-GFP fluorescence measurements after different time of cell cultivation, (**D**) Intracellular location of Hxt6-GFP signal determined by fluorescence microscopy after different time of cell cultivation, (**E**) Transcription of the low-affinity hexose transporter gene *HXT1* in the WT yeast cells grown on medium with glucose or fructose, (**F**) Transcription of the high-affinity hexose transporter gene *HXT6* in the WT yeast cells grown on medium with glucose or fructose, (**G**) The rate of carbohydrate utilization by WT yeast cells grown in glucose or fructose conditions determined by measurements of glucose or fructose concentration in medium after 12, 16, 20, 24 h of cell cultivation. The results are presented as mean ± SD from at least three independent experiments. Hxts-GFP were visualized using fluorescence microscope Olympus BX-51 equipped with the DP-72 digital camera and cellSens Dimension v1.0 software at appropriate wavelengths. The microscopic images present typical results from of the duplicate experiment. Magnification 100×. * $p < 0.05$; *** $p < 0.001$ as compared between media with glucose and fructose; a – different to exponential phase of yeast cell growth, b - different to stationary phase of yeast cell growth, c - different to 2 days of yeast cell cultivation.

Figure 4. ***Parameters connected with biosynthetic capabilities and the action of the pentose-phosphate pathway in WT yeast cells cultured in medium with glucose or fructose*** (**A**) Relative Zwf1p level quantified by Zwf1-GFP fluorescence measurements in the WT yeast cells grown on medium with glucose or fructose, (**B**) Intracellular location of Zwf1-GFP signal determined by fluorescence microscopy in the WT yeast cells grown on medium with glucose or fructose, (**C**) Transcription of the *ZWF1* gene in the WT yeast cells grown on medium with glucose or fructose, (**D**) The content of glucose-6-phosphate (G6P) determined in deproteinized cell extracts (10 kDa MWCO) using Glucose-6-Phosphate Assay, (**E**) PP pathway enzymes activity: glucose-6-phosphate dehydrogenase (G6PD) and 6-phosphogluconate dehydrogenase (6-PGD) determined spectrophotometrically by measuring the rate of $NADP^+$ reduction at 340 nm, (**F**) Protein content in cell extracts obtained from a strictly defined number of cells (5×10^8 yeast cells from the exponential phase culture) expressed in the pg per cell. The results are presented as mean ± SD from at least three independent experiments. Zwf1-GFP were visualized using fluorescence microscope Olympus BX-51 equipped with the DP-72 digital camera and cellSens Dimension v1.0 software at appropriate wavelengths The microscopic images present typical results from of the duplicate experiment. Magnification 100×. * $p < 0.05$; *** $p < 0.01$; *** $p < 0.001$ as compared between media with glucose and fructose.

Figure 5. ***Parameters connected with mitochondrial function and metabolism in WT yeast cells cultured in medium with glucose or fructose*** (**A**) Mitochondrial membrane potential (MMP) and (**B**) morphology of the mitochondrial network determined using rhodamine B hexyl ester. The fluorescence was measured at λ_{ex} = 555 nm and λ_{em} = 579 nm. Mitochondrial network was visualized using fluorescence microscope Olympus BX-51 equipped with the DP-72 digital camera and cellSens Dimension v1.0 software at appropriate wavelengths. The microscopic images present typical results from of the duplicate experiment. Magnification 100×, (**C**) Intracellular ATP content in the WT yeast cells grown on medium with glucose or fructose determined with BacTiter-Glo™ Microbial Cell Viability Assay, (**D**) The ATP level, (**E**) ADP level, (**F**) ADP+ATP pool and (**G**) ATP/ADP ratio measured in whole cell extract using ADP/ATP Ratio Assay Kit, (**H**) The ROS content in the WT strain cultivated on medium with glucose or fructose estimated by the rate of fluorescence increase due to dihydroethidium (DHET) oxidation within cells. The fluorescence was measured at λ_{ex} = 518 nm, λ_{em} = 605 nm, (**I**) The level of cAMP in the WT yeast cells grown on medium with glucose or fructose determined with Direct cAMP Elisa kit in acetylated format. The absorbance was measured at λ = 405 nm. The amount of cAMP in the samples was expressed as pmol per mg of total protein.

The results are presented as mean ± SD from at least three independent experiments. * $p < 0.05$; *** $p < 0.01$; *** $p < 0.001$ as compared between media with glucose and fructose.

Figure 6. ***Parameters connected with mitochondrial function and metabolism in WT and Δhxk2 yeast strains cultured in medium with glucose or fructose*** (**A**) Mitochondrial membrane potential (MMP) and (**B**) morphology of the mitochondrial network determined using rhodamine B hexyl ester. The fluorescence was measured at λ_{ex} = 555 nm and λ_{em} = 579 nm. Mitochondrial network was visualized using fluorescence microscope Olympus BX-51 equipped with the DP-72 digital camera and cellSens Dimension v1.0 software at appropriate wavelengths. The microscopic images present typical results from of the duplicate experiment. Magnification 100×, (**C**) Intracellular ATP content in the WT yeast cells grown on medium with glucose or fructose determined with BacTiter-Glo™ Microbial Cell Viability Assay, (**D**) The ATP level, (**E**) ADP level, (**F**) ADP+ATP pool and (**G**) ATP/ADP ratio measured in whole cell extract using ADP/ATP Ratio Assay Kit, (**H**) The ROS content in the WT strain cultivated on medium with glucose or fructose estimated by the rate of fluorescence increase due to dihydroethidium (DHET) oxidation within cells. The fluorescence was measured at λ_{ex} = 518 nm, λ_{em} = 605 nm, (**I**) The level of cAMP in the WT yeast cells grown on medium with glucose or fructose determined with Direct cAMP Elisa kit in acetylated format. The absorbance was measured at λ = 405 nm. The amount of cAMP in the samples was expressed as pmol per mg of total protein. The results are presented as mean ± SD from at least three independent experiments. * $p < 0.05$; *** $p < 0.01$; *** $p < 0.001$ as compared between media with glucose and fructose; $^{\#}$ $p < 0.05$, $^{\#\#}$ $p < 0.01$, $^{\#\#\#}$ $p < 0.001$ as compared to WT strain cultivated in a glucose medium.

Figure 7. The changes in the level of ATP and ROS content in WT and Δhxk2 yeast strains cultured in medium with glucose or fructose after cell incubation with mitochondria respiration inhibitors. (**A**) Changes in ATP content and (**B**) changes in ROS content in grown on medium with glucose or fructose after 30 min incubations with 60 μM Antimycin A or 30 μM Oligomycin. The ATP level was determined by luminescence measurements using BacTiter-Glo™ Microbial Cell Viability Assay. The ROS content was estimated by the rate of fluorescence increase due to dihydroethidium (DHET) oxidation within cells. The results are presented as mean ± SD from at least three independent experiments. * $p < 0.05$; *** $p < 0.01$; *** $p < 0.001$ as compared between media with glucose and fructose; $^{\#}$ $p < 0.05$, $^{\#\#}$ $p < 0.01$, $^{\#\#\#}$ $p < 0.001$ as compared to WT strain cultivated in a glucose medium.

Figure 8. ***Parameters connected with carbohydrate uptake, biosynthetic capabilities and the action of the pentose-phosphate pathway in WT and Δhxk2 yeast strains cultured in medium with glucose or fructose*** (**A**) The rate of glucose uptake by yeast cells of WT and Δ*hxk2* strains. Quantification of relative glucose uptake was performed by measuring the fluorescent signal after incubation with 6-NBDG, (**B**) Transcription of the low-affinity hexose transporter gene *HXT1* in the WT and Δ*hxk2* yeast cells grown on medium with glucose or fructose, (**C**) Transcription of the high-affinity hexose transporter gene *HXT6* in the WT and Δ*hxk2* yeast cells grown on medium with glucose or fructose, (**D**) The rate of carbohydrate utilization by WT and Δ*hxk2* yeast cells grown in glucose or fructose conditions determined by measurements of glucose or fructose concentration in medium after 12, 16, 20, 24 h of cell cultivation, (**E**) The content of glucose-6-phosphate (G6P) determined in deproteinized cell extracts from the WT and Δ*hxk2* yeast cells grown on medium with glucose or fructose, (**F**) PP pathway enzymes activity: glucose-6-phosphate dehydrogenase (G6PD) and 6-phosphogluconate dehydrogenase (6-PGD) determined for the WT and Δ*hxk2* yeast cells grown on medium with glucose or fructose by measuring the rate of $NADP^+$ reduction at 340 nm, (**G**) Transcription of the *ZWF1* gene in the WT and Δ*hxk2* yeast cells grown on medium with glucose or fructose, (**H**) Protein content in cell extracts obtained from the WT and Δ*hxk2* yeast cells grown on medium with glucose or fructose. Data expressed in the pg per cell. The results are presented as mean ± SD from at least three independent experiments. * $p < 0.05$; ** $p < 0.01$; *** $p < 0.001$ as compared between media with glucose and fructose; $^{\#}$ $p < 0.05$, $^{\#\#}$ $p < 0.01$, $^{\#\#\#}$ $p < 0.001$ as compared to WT strain cultivated in a glucose medium.

Figure 9. ***The growth of WT and Δhxk2 yeast strains cultured in medium with glucose or fructose*** (**A**) Growth kinetic of yeast cell population of WT and Δ*hxk2* strains monitored during 12 h, (**B**) The growth rate of WT and Δ*hxk2* yeast strains, (**C**) The growth of the yeast cell population of WT and Δ*hxk2* strains monitored after 24 h and 36 h. The results are presented as mean ± SD from three independent experiments. * $p < 0.05$; ** $p < 0.01$ as compared between media with glucose and fructose; $^{\#}$ $p < 0.05$, $^{\#\#}$ $p < 0.01$, $^{\#\#\#}$ $p < 0.001$ as compared to WT strain cultivated in a glucose medium.

Figure 10. ***The reproductive potential of WT and Δhxk2 yeast strains cultured in medium with glucose or fructose*** (**A**) The reproductive potential of yeast cells of WT and Δ*hxk2* strains growing in glucose or fructose conditions, (**B**) Distribution of reproductive potential in population of yeast cell of WT and Δ*hxk2* strains growing in glucose or fructose conditions, (**C**) Maximal reproductive potential determined for WT and Δ*hxk2* strains growing in glucose

or fructose conditions. Maximal reproductive potential was determined on the basis of 10% yeast cells with the highest number of daughters cells. The data represent the mean values from two independent experiments of 40 cells each. * $p < 0.05$; *** $p < 0.001$ as compared between media with glucose and fructose; $^{\#}$ $p < 0.05$, $^{\#\#\#}$ $p < 0.001$ as compared to WT strain cultivated in a glucose medium.

Supplementary figure 1. The carbohydrate concentrations obtained for yeast strains carrying GFP-proteins cultured in medium with glucose or fructose. Glucose or fructose concentration in the culture medium was determined at exponential phase, stationary phase and after 2 days of cell cultivation. The results are presented as mean ± SD from at least three independent experiments.

Supplementary figure 2. Relative Zwf1p level and intracellular location of Zwf1-GFP signal determined after different time of cell cultivation on medium with glucose or fructose. Zwf1p level was quantified by Zwf1-GFP fluorescence measurements and intracellular location of Zwf1-GFP signal was determined by fluorescence microscopy. Both parameters were determined at exponential phase, stationary phase and after 2 days of cell cultivation. The results are presented as mean ± SD from at least three independent experiments. Zwf1-GFP were visualized using fluorescence microscope Olympus BX-51 equipped with the DP-72 digital camera and cellSens Dimension v1.0 software at appropriate wavelengths The microscopic images present typical results from of the duplicate experiment. Magnification 100×. * $p < 0.05$ as compared between media with glucose and fructose; a – different to exponential phase of yeast cell growth, b - different to stationary phase of yeast cell growth, c - different to 2 days of yeast cell cultivation.

References

[1] S. Busti, P. Coccetti, L. Alberghina, M. Vanoni, Glucose signaling-mediated coordination of cell growth and cell cycle in *Saccharomyces cerevisiae*, Sensors (Basel) 10(6) (2010) 6195-240.

[2] M.G. Vander Heiden, L.C. Cantley, C.B. Thompson, Understanding the Warburg effect: the metabolic requirements of cell proliferation, Science 324(5930) (2009) 1029-33.

[3] A. Bloem, I. Sanchez, S. Dequin, C. Camarasa, Metabolic Impact of Redox Cofactor Perturbations on the Formation of Aroma Compounds in *Saccharomyces cerevisiae*, Appl Environ Microbiol 82(1) (2016) 174-83.

[4] C.D. Folmes, A. Terzic, Energy metabolism in the acquisition and maintenance of stemness, Semin Cell Dev Biol 52 (2016) 68-75.

[5] D. Molenaar, R. van Berlo, D. de Ridder, B. Teusink, Shifts in growth strategies reflect tradeoffs in cellular economics, Mol Syst Biol 5 (2009) 323.

[6] A. Nilsson, J. Nielsen, Metabolic Trade-offs in Yeast are Caused by F1F0-ATP synthase, Sci Rep 6 (2016) 22264.

[7] R. Maslanka, R. Zadrag-Tecza, Different life strategies in genetic backgrounds of the *Saccharomyces cerevisiae* yeast cells, Fungal Biol 126(8) (2022) 498-510.

[8] T. Nidelet, P. Brial, C. Camarasa, S. Dequin, Diversity of flux distribution in central carbon metabolism of *S. cerevisiae* strains from diverse environments, Microb Cell Fact 15 (2016) 58.

[9] A. Spor, T. Nidelet, J. Simon, A. Bourgais, D. de Vienne, D. Sicard, Niche-driven evolution of metabolic and life-history strategies in natural and domesticated populations of *Saccharomyces cerevisiae*, BMC Evol Biol 9 (2009) 296.

[10] A. Spor, S. Wang, C. Dillmann, D. de Vienne, D. Sicard, "Ant" and "grasshopper" life-history strategies in *Saccharomyces cerevisiae*, PLoS One 3(2) (2008) e1579.

[11] M. Rigoulet, C.L. Bouchez, P. Paumard, S. Ransac, S. Cuvellier, S. Duvezin-Caubet, J.P. Mazat, A. Devin, Cell energy metabolism: An update, Biochim Biophys Acta Bioenerg 1861(11) (2020) 148276.

[12] N. Gasmi, P.E. Jacques, N. Klimova, X. Guo, A. Ricciardi, F. Robert, B. Turcotte, The switch from fermentation to respiration in *Saccharomyces cerevisiae* is regulated by the Ert1 transcriptional activator/repressor, Genetics 198(2) (2014) 547-60.

[13] S. Ohlmeier, A.J. Kastaniotis, J.K. Hiltunen, U. Bergmann, The yeast mitochondrial proteome, a study of fermentative and respiratory growth, J Biol Chem 279(6) (2004) 3956-79.

[14] G.G. Roberts, A.P. Hudson, Transcriptome profiling of *Saccharomyces cerevisiae* during a transition from fermentative to glycerol-based respiratory growth reveals extensive metabolic and structural remodeling, Mol Genet Genomics 276(2) (2006) 170-86.

[15] K. Shimizu, Y. Matsuoka, Regulation of glycolytic flux and overflow metabolism depending on the source of energy generation for energy demand, Biotechnol Adv 37(2) (2019) 284-305.

[16] F. Di Bartolomeo, C. Malina, K. Campbell, M. Mormino, J. Fuchs, E. Vorontsov, C.M. Gustafsson, J. Nielsen, Absolute yeast mitochondrial proteome quantification reveals trade-off between biosynthesis and energy generation during diauxic shift, Proc Natl Acad Sci U S A 117(13) (2020) 7524-7535.

[17] M. Malecki, S. Kamrad, M. Ralser, J. Bähler, Mitochondrial respiration is required to provide amino acids during fermentative proliferation of fission yeast, EMBO Rep 21(11) (2020) e50845.

[18] R. Diaz-Ruiz, M. Rigoulet, A. Devin, The Warburg and Crabtree effects: On the origin of cancer cell energy metabolism and of yeast glucose repression, Biochim Biophys Acta 1807(6) (2011) 568-76.

[19] O. Warburg, On the origin of cancer cells, Science 123(3191) (1956) 309-14.

[20] C. Hu, L. Fan, P. Cen, E. Chen, Z. Jiang, L. Li, Energy Metabolism Plays a Critical Role in Stem Cell Maintenance and Differentiation, Int J Mol Sci 17(2) (2016) 253.

[21] R.H. De Deken, The Crabtree effect: a regulatory system in yeast, J Gen Microbiol 44(2) (1966) 149-56.

[22] A. Hagman, T. Säll, J. Piškur, Analysis of the yeast short-term Crabtree effect and its origin, FEBS J 281(21) (2014) 4805-14.

[23] S.V. Rødkaer, N.J. Faergeman, Glucose- and nitrogen sensing and regulatory mechanisms in *Saccharomyces cerevisiae*, FEMS Yeast Res 14(5) (2014) 683-96.

[24] V.D. Longo, The Ras and Sch9 pathways regulate stress resistance and longevity, Exp Gerontol 38(7) (2003) 807-11.

[25] F. Rolland, J. Winderickx, J.M. Thevelein, Glucose-sensing and -signalling mechanisms in yeast, FEMS Yeast Res 2(2) (2002) 183-201.

[26] K. Peeters, F. Van Leemputte, B. Fischer, B.M. Bonini, H. Quezada, M. Tsytlonok, D. Haesen, W. Vanthienen, N. Bernardes, C.B. Gonzalez-Blas, V. Janssens, P. Tompa, W.

Versées, J.M. Thevelein, Fructose-1,6-bisphosphate couples glycolytic flux to activation of Ras, Nat Commun 8(1) (2017) 922.

[27] M. Vega, A. Riera, A. Fernández-Cid, P. Herrero, F. Moreno, Hexokinase 2 Is an Intracellular Glucose Sensor of Yeast Cells That Maintains the Structure and Activity of Mig1 Protein Repressor Complex, J Biol Chem 291(14) (2016) 7267-85.

[28] A. Rodríguez, T. De La Cera, P. Herrero, F. Moreno, The hexokinase 2 protein regulates the expression of the GLK1, HXK1 and HXK2 genes of *Saccharomyces cerevisiae*, Biochem J 355(Pt 3) (2001) 625-31.

[29] S.J. Lin, P.A. Defossez, L. Guarente, Requirement of NAD and SIR2 for life-span extension by calorie restriction in *Saccharomyces cerevisiae*, Science 289(5487) (2000) 2126-8.

[30] R. Maslanka, R. Zadrag-Tecza, Reproductive Potential of Yeast Cells Depends on Overall Action of Interconnected Changes in Central Carbon Metabolism, Cellular Biosynthetic Capacity, and Proteostasis, Int J Mol Sci 21(19) (2020).

[31] R. Maslanka, M. Kwolek-Mirek, R. Zadrag-Tecza, Consequences of calorie restriction and calorie excess for the physiological parameters of the yeast *Saccharomyces cerevisiae* cells, FEMS Yeast Res 17(8) (2017).

[32] R. Maslanka, R. Zadrag-Tecza, Less is more or more is less: Implications of glucose metabolism in the regulation of the reproductive potential and total lifespan of the *Saccharomyces cerevisiae* yeast, J Cell Physiol 234(10) (2019) 17622-17638.

[33] C. Guillaume, P. Delobel, J.M. Sablayrolles, B. Blondin, Molecular basis of fructose utilization by the wine yeast *Saccharomyces cerevisiae*: a mutated HXT3 allele enhances fructose fermentation, Appl Environ Microbiol 73(8) (2007) 2432-9.

[34] P. Hapeta, P. Szczepańska, T. Witkowski, J.M. Nicaud, A.M. Crutz-Le Coq, Z. Lazar, The Role of Hexokinase and Hexose Transporters in Preferential Use of Glucose over Fructose and Downstream Metabolic Pathways in the Yeast, Int J Mol Sci 22(17) (2021).

[35] L. Mocke, Kinetic Modelling of Wine Fermentations: Why Does Yeast Prefer Glucose to Fructose?, Department of Biochemistry, University of Stellenbosch, Matieland 7602, South Afica, 2013, pp. 1-64.

[36] N.J. Berthels, R.R. Cordero Otero, F.F. Bauer, J.M. Thevelein, I.S. Pretorius, Discrepancy in glucose and fructose utilisation during fermentation by *Saccharomyces cerevisiae* wine yeast strains, FEMS Yeast Res 4(7) (2004) 683-9.

[37] H.M. Semchyshyn, L.M. Lozinska, Fructose protects baker's yeast against peroxide stress: potential role of catalase and superoxide dismutase, FEMS Yeast Res 12(7) (2012) 761-73.

[38] H.M. Semchyshyn, L.M. Lozinska, J. Miedzobrodzki, V.I. Lushchak, Fructose and glucose differentially affect aging and carbonyl/oxidative stress parameters in *Saccharomyces cerevisiae* cells, Carbohydr Res 346(7) (2011) 933-8.

[39] W.K. Huh, J.V. Falvo, L.C. Gerke, A.S. Carroll, R.W. Howson, J.S. Weissman, E.K. O'Shea, Global analysis of protein localization in budding yeast, Nature 425(6959) (2003) 686-91.

[40] J. Wawryn, A. Krzepiłko, A. Myszka, T. Biliński, Deficiency in superoxide dismutases shortens life span of yeast cells, Acta Biochim Pol 46(2) (1999) 249-53.

[41] R. Zadrag, G. Bartosz, T. Bilinski, Is the yeast a relevant model for aging of multicellular organisms? An insight from the total lifespan of *Saccharomyces cerevisiae*, Curr Aging Sci 1(3) (2008) 159-65.

[42] D.L. Maskell, A.I. Kennedy, J.A. Hodgson, K.A. Smart, Chronological and replicative lifespan of polyploid *Saccharomyces cerevisiae* (syn. *S. pastorianus*), FEMS Yeast Res 3(2) (2003) 201-9.

[43] J. Vijg, E. Le Bourg, Aging and the Inevitable Limit to Human Life Span, Gerontology 63(5) (2017) 432-434.

[44] F. Widdel, Theory and measurement of bacterial growth, Di dalam Grundpraktikum Mikrobiologie 4(11) (2007).

[45] W.N. Tian, L.D. Braunstein, J. Pang, K.M. Stuhlmeier, Q.C. Xi, X. Tian, R.C. Stanton, Importance of glucose-6-phosphate dehydrogenase activity for cell growth, J Biol Chem 273(17) (1998) 10609-17.

[46] M. Takaine, H. Imamura, S. Yoshida, High and stable ATP levels prevent aberrant intracellular protein aggregation in yeast, Elife 11 (2022).

[47] N.J. Berthels, R.R. Cordero Otero, F.F. Bauer, I.S. Pretorius, J.M. Thevelein, Correlation between glucose/fructose discrepancy and hexokinase kinetic properties in different *Saccharomyces cerevisiae* wine yeast strains, Appl Microbiol Biotechnol 77(5) (2008) 1083-91.

[48] Z. Lazar, A. Dobrowolski, M. Robak, [Fructose transporter in yeasts], Postepy Biochem 60(1) (2014) 94-101.

[49] L.F. Montaño-Gutierrez, K. Correia, P.S. Swain, Multiple nutrient transporters enable cells to mitigate a rate-affinity tradeoff, PLoS Comput Biol 18(4) (2022) e1010060.

[50] S. Krampe, O. Stamm, C.P. Hollenberg, E. Boles, Catabolite inactivation of the high-affinity hexose transporters Hxt6 and Hxt7 of *Saccharomyces cerevisiae* occurs in the vacuole after internalization by endocytosis, FEBS Lett 441(3) (1998) 343-7.

[51] A. Yoshida, D. Wei, W. Nomura, S. Izawa, Y. Inoue, Reduction of glucose uptake through inhibition of hexose transporters and enhancement of their endocytosis by methylglyoxal in *Saccharomyces cerevisiae*, J Biol Chem 287(1) (2012) 701-711.

[52] T. Biliński, R. Zadrąg-Tęcza, G. Bartosz, Hypertrophy hypothesis as an alternative explanation of the phenomenon of replicative aging of yeast, FEMS Yeast Res 12(1) (2012) 97-101.

[53] D.M. Davies, K. van den Handel, S. Bharadwaj, J. Lengefeld, Cellular enlargement - A new hallmark of aging?, Front Cell Dev Biol 10 (2022) 1036602.

[54] G.E. Neurohr, R.L. Terry, J. Lengefeld, M. Bonney, G.P. Brittingham, F. Moretto, T.P. Miettinen, L.P. Vaites, L.M. Soares, J.A. Paulo, J.W. Harper, S. Buratowski, S. Manalis, F.J. van Werven, L.J. Holt, A. Amon, Excessive Cell Growth Causes Cytoplasm Dilution And Contributes to Senescence, Cell 176(5) (2019) 1083-1097.e18.

[55] R. Zadrag-Tecza, M. Kwolek-Mirek, M. Alabrudzińska, A. Skoneczna, Cell Size Influences the Reproductive Potential and Total Lifespan of the, Oxid Med Cell Longev 2018 (2018) 1898421.

[56] J.J. Lemasters, Metabolic implications of non-electrogenic ATP/ADP exchange in cancer cells: A mechanistic basis for the Warburg effect, Biochim Biophys Acta Bioenerg 1862(7) (2021) 148410.

[57] E.N. Maldonado, J.J. Lemasters, ATP/ADP ratio, the missed connection between mitochondria and the Warburg effect, Mitochondrion 19 Pt A (2014) 78-84.

[58] A. Kümmel, J.C. Ewald, S.M. Fendt, S.J. Jol, P. Picotti, R. Aebersold, U. Sauer, N. Zamboni, M. Heinemann, Differential glucose repression in common yeast strains in response to *HXK2* deletion, FEMS Yeast Res 10(3) (2010) 322-32.

[59] S.J. Lin, M. Kaeberlein, A.A. Andalis, L.A. Sturtz, P.A. Defossez, V.C. Culotta, G.R. Fink, L. Guarente, Calorie restriction extends *Saccharomyces cerevisiae* lifespan by increasing respiration, Nature 418(6895) (2002) 344-8.

[60] D. Harman, Aging: a theory based on free radical and radiation chemistry, J Gerontol 11(3) (1956) 298-300.

[61] C. Lennicke, H.M. Cochemé, Redox metabolism: ROS as specific molecular regulators of cell signaling and function, Mol Cell 81(18) (2021) 3691-3707.

[62] M. Rinnerthaler, S. Büttner, P. Laun, G. Heeren, T.K. Felder, H. Klinger, M. Weinberger, K. Stolze, T. Grousl, J. Hasek, O. Benada, I. Frydlova, A. Klocker, B. Simon-Nobbe, B. Jansko, H. Breitenbach-Koller, T. Eisenberg, C.W. Gourlay, F. Madeo, W.C. Burhans, M. Breitenbach, Yno1p/Aim14p, a NADPH-oxidase ortholog, controls extramitochondrial reactive oxygen species generation, apoptosis, and actin cable formation in yeast, Proc Natl Acad Sci U S A 109(22) (2012) 8658-63.

[63] T. Biliński, T. Paszkiewicz, R. Zadrag-Tecza, Energy excess is the main cause of accelerated aging of mammals, Oncotarget 6(15) (2015) 12909-19.

[64] D. Lee, H.G. Son, Y. Jung, S.V. Lee, The role of dietary carbohydrates in organismal aging, Cell Mol Life Sci 74(10) (2017) 1793-1803.

[65] J.C. Mathers, Impact of nutrition on the ageing process, Br J Nutr 113 Suppl (2015) S18-22.

[66] S.A. Hannou, D.E. Haslam, N.M. McKeown, M.A. Herman, Fructose metabolism and metabolic disease, J Clin Invest 128(2) (2018) 545-555.

[67] M.A. Herman, M.J. Birnbaum, Molecular aspects of fructose metabolism and metabolic disease, Cell Metab 33(12) (2021) 2329-2354.

[68] D. Lodha, S. Rajasekaran, T. Jayavelu, J.R. Subramaniam, Detrimental effects of fructose on mitochondria in mouse motor neurons and on, Nutr Neurosci 25(6) (2022) 1277-1286.

[69] D.L. Maskell, A.I. Kennedy, J.A. Hodgson, K.A. Smart, Impact of Carbohydrate Composition of Media on Lager Yeast Replicative Lifespan, Journal of the American Society of Brewing Chemists 59(3) (2001) 111-116.

[70] M. Tsuchiya, N. Dang, E.O. Kerr, D. Hu, K.K. Steffen, J.A. Oakes, B.K. Kennedy, M. Kaeberlein, Sirtuin-independent effects of nicotinamide on lifespan extension from calorie restriction in yeast, Aging Cell 5(6) (2006) 505-14.

[71] A. Litsios, D.H.E.W. Huberts, H.M. Terpstra, P. Guerra, A. Schmidt, K. Buczak, A. Papagiannakis, M. Rovetta, J. Hekelaar, G. Hubmann, M. Exterkate, A. Milias-Argeitis, M. Heinemann, Differential scaling between G1 protein production and cell size dynamics promotes commitment to the cell division cycle in budding yeast, Nat Cell Biol 21(11) (2019) 1382-1392.

[72] C. Malina, R. Yu, J. Björkeroth, E.J. Kerkhoven, J. Nielsen, Adaptations in metabolism and protein translation give rise to the Crabtree effect in yeast, Proc Natl Acad Sci U S A 118(51) (2021).

[73] M. Perez, K. Luyten, R. Michel, C. Riou, B. Blondin, Analysis of *Saccharomyces cerevisiae* hexose carrier expression during wine fermentation: both low- and high-affinity Hxt transporters are expressed, FEMS Yeast Res 5(4-5) (2005) 351-61.

[74] A. Carrillo-Garmendia, C. Martinez-Ortiz, J.G. Martinez-Garfias, S.E. Suarez-Sandoval, J.C. González-Hernández, G.M. Nava, M.D. Dufoo-Hurtado, L.A. Madrigal-Perez, Snf1p/Hxk2p/Mig1p pathway regulates hexose transporters transcript levels, affecting the exponential growth and mitochondrial respiration of *Saccharomyces cerevisiae*, Fungal Genet Biol 161 (2022) 103701.

[75] J. Roosen, C. Oesterhelt, K. Pardons, E. Swinnen, J. Winderickx, Integration of nutrient signalling pathways in the yeast *Saccharomyces cerevisiae*, in: J. Winderickx, P.M. Taylor (Eds.), Topics in current genetics. Nutrient-induced responses in eukaryotic cells, Springer, Heidelberg, 2004, pp. 277–318.

[76] D. Botman, T.G. O'Toole, J. Goedhart, F.J. Bruggeman, J.H. van Heerden, B. Teusink, A yeast FRET biosensor enlightens cAMP signaling, Mol Biol Cell 32(13) (2021) 1229-1240.

[77] T. Schmelzle, T. Beck, D.E. Martin, M.N. Hall, Activation of the RAS/cyclic AMP pathway suppresses a TOR deficiency in yeast, Mol Cell Biol 24(1) (2004) 338-51.

[78] J.M. Gancedo, The early steps of glucose signalling in yeast, FEMS Microbiol Rev 32(4) (2008) 673-704.

[79] L.L. Newcomb, J.A. Diderich, M.G. Slattery, W. Heideman, Glucose regulation of *Saccharomyces cerevisiae* cell cycle genes, Eukaryot Cell 2(1) (2003) 143-9.

[80] M.G. Mirisola, V.D. Longo, Yeast Chronological Lifespan: Longevity Regulatory Genes and Mechanisms, Cells 11(10) (2022).

[81] J.E. Leadsham, C.W. Gourlay, cAMP/PKA signaling balances respiratory activity with mitochondria dependent apoptosis via transcriptional regulation, BMC Cell Biol 11 (2010) 92.

[82] H. Safdari, A. Kalirad, M. Sadeghi, Population-level heterogeneity as a reflection of mixed strategy: A computational perspective on the Crabtree effect, J Theor Biol 531 (2021) 110912.

[83] E. de Alteriis, F. Cartenì, P. Parascandola, J. Serpa, S. Mazzoleni, Revisiting the Crabtree/Warburg effect in a dynamic perspective: a fitness advantage against sugar-induced cell death, Cell Cycle 17(6) (2018) 688-701.

[84] M. Rosas Lemus, E. Roussarie, N. Hammad, A. Mougeolle, S. Ransac, R. Issa, J.P. Mazat, S. Uribe-Carvajal, M. Rigoulet, A. Devin, The role of glycolysis-derived hexose

phosphates in the induction of the Crabtree effect, J Biol Chem 293(33) (2018) 12843-12854.

[85] J.A. Diderich, L.M. Raamsdonk, A.L. Kruckeberg, J.A. Berden, K. Van Dam, Physiological properties of *Saccharomyces cerevisiae* from which hexokinase II has been deleted, Appl Environ Microbiol 67(4) (2001) 1587-93.

[86] D. Guo, Y. Meng, X. Jiang, Z. Lu, Hexokinases in cancer and other pathologies, Cell Insight 2(1) (2023) 100077.

[87] Y. Chen, J. Nielsen, Energy metabolism controls phenotypes by protein efficiency and allocation, Proc Natl Acad Sci U S A 116(35) (2019) 17592-17597.

[88] R. Maslanka, M. Kwolek-Mirek, R. Zadrag-Tecza, Autofluorescence of yeast *Saccharomyces cerevisiae* cells caused by glucose metabolism products and its methodological implications, J Microbiol Methods 146 (2018) 55-60.

[89] R.C. Stanton, Glucose-6-phosphate dehydrogenase, NADPH, and cell survival, IUBMB Life 64(5) (2012) 362-9.

[90] Z. Hu, B. Xia, S.D. Postnikoff, Z.J. Shen, A.S. Tomoiaga, T.A. Harkness, J.H. Seol, W. Li, K. Chen, J.K. Tyler, Ssd1 and Gcn2 suppress global translation efficiency in replicatively aged yeast while their activation extends lifespan, Elife 7 (2018).

[91] G.E. Janssens, A.C. Meinema, J. González, J.C. Wolters, A. Schmidt, V. Guryev, R. Bischoff, E.C. Wit, L.M. Veenhoff, M. Heinemann, Protein biogenesis machinery is a driver of replicative aging in yeast, Elife 4 (2015) e08527.

[92] Y.C. Chen, P.H. Jiang, H.M. Chen, C.H. Chen, Y.T. Wang, Y.J. Chen, C.J. Yu, S.C. Teng, Glucose intake hampers PKA-regulated HSP90 chaperone activity, Elife 7 (2018).

[93] Y. Yuan, J.Y. Lin, H.J. Cui, W. Zhao, H.L. Zheng, Z.W. Jiang, X.D. Xiong, S. Xu, X.G. Liu, PCK1 Deficiency Shortens the Replicative Lifespan of *Saccharomyces cerevisiae* through Upregulation of PFK1, Biomed Res Int 2020 (2020) 3858465.

[94] M.H. Barros, B. Bandy, E.B. Tahara, A.J. Kowaltowski, Higher respiratory activity decreases mitochondrial reactive oxygen release and increases life span in *Saccharomyces cerevisiae*, J Biol Chem 279(48) (2004) 49883-8.

[95] S.J. Lin, E. Ford, M. Haigis, G. Liszt, L. Guarente, Calorie restriction extends yeast life span by lowering the level of NADH, Genes Dev 18(1) (2004) 12-6.

[96] E.B. Tahara, F.M. Cunha, T.O. Basso, B.E. Della Bianca, A.K. Gombert, A.J. Kowaltowski, Calorie restriction hysteretically primes aging *Saccharomyces cerevisiae* toward more effective oxidative metabolism, PLoS One 8(2) (2013) e56388.

[97] A. Ocampo, J. Liu, E.A. Schroeder, G.S. Shadel, A. Barrientos, Mitochondrial respiratory thresholds regulate yeast chronological life span and its extension by caloric restriction, Cell Metab 16(1) (2012) 55-67.

[98] M. Kaeberlein, D. Hu, E.O. Kerr, M. Tsuchiya, E.A. Westman, N. Dang, S. Fields, B.K. Kennedy, Increased life span due to calorie restriction in respiratory-deficient yeast, PLoS Genet 1(5) (2005) e69.

[99] D.K. Woo, R.O. Poyton, The absence of a mitochondrial genome in rho0 yeast cells extends lifespan independently of retrograde regulation, Exp Gerontol 44(6-7) (2009) 390-7.

[100] W. Yang, S. Hekimi, A mitochondrial superoxide signal triggers increased longevity in *Caenorhabditis elegans*, PLoS Biol 8(12) (2010) e1000556.

[101] J. Pan, Q. Chang, X. Wang, Y. Son, Z. Zhang, G. Chen, J. Luo, Y. Bi, F. Chen, X. Shi, Reactive oxygen species-activated Akt/ASK1/p38 signaling pathway in nickel compound-induced apoptosis in BEAS 2B cells, Chem Res Toxicol 23(3) (2010) 568-77.

[102] T. Burphan, S. Tatip, T. Limcharoensuk, K. Kangboonruang, C. Boonchird, C. Auesukaree, Enhancement of ethanol production in very high gravity fermentation by reducing fermentation-induced oxidative stress in *Saccharomyces cerevisiae*, Sci Rep 8(1) (2018) 13069.

[103] S. Busti, V. Mapelli, F. Tripodi, R. Sanvito, F. Magni, P. Coccetti, M. Rocchetti, J. Nielsen, L. Alberghina, M. Vanoni, Respiratory metabolism and calorie restriction relieve persistent endoplasmic reticulum stress induced by calcium shortage in yeast, Sci Rep 6 (2016) 27942.

[104] P. Pawelczak, A. Fedoruk-Wyszomirska, E. Wyszko, Antiaging Effect of 4, Antioxidants (Basel) 11(5) (2022).

[105] D.G. Yi, S. Hong, W.K. Huh, Mitochondrial dysfunction reduces yeast replicative lifespan by elevating RAS-dependent ROS production by the ER-localized NADPH oxidase Yno1, PLoS One 13(6) (2018) e0198619.

[106] M.P. Mori, R. Penjweini, J. Ma, G. Alspaugh, A. Andreoni, Y.C. Kim, P.Y. Wang, J.R. Knutson, P.M. Hwang, Mitochondrial respiration reduces exposure of the nucleus to oxygen, J Biol Chem 299(3) (2023) 103018.

Figure 1

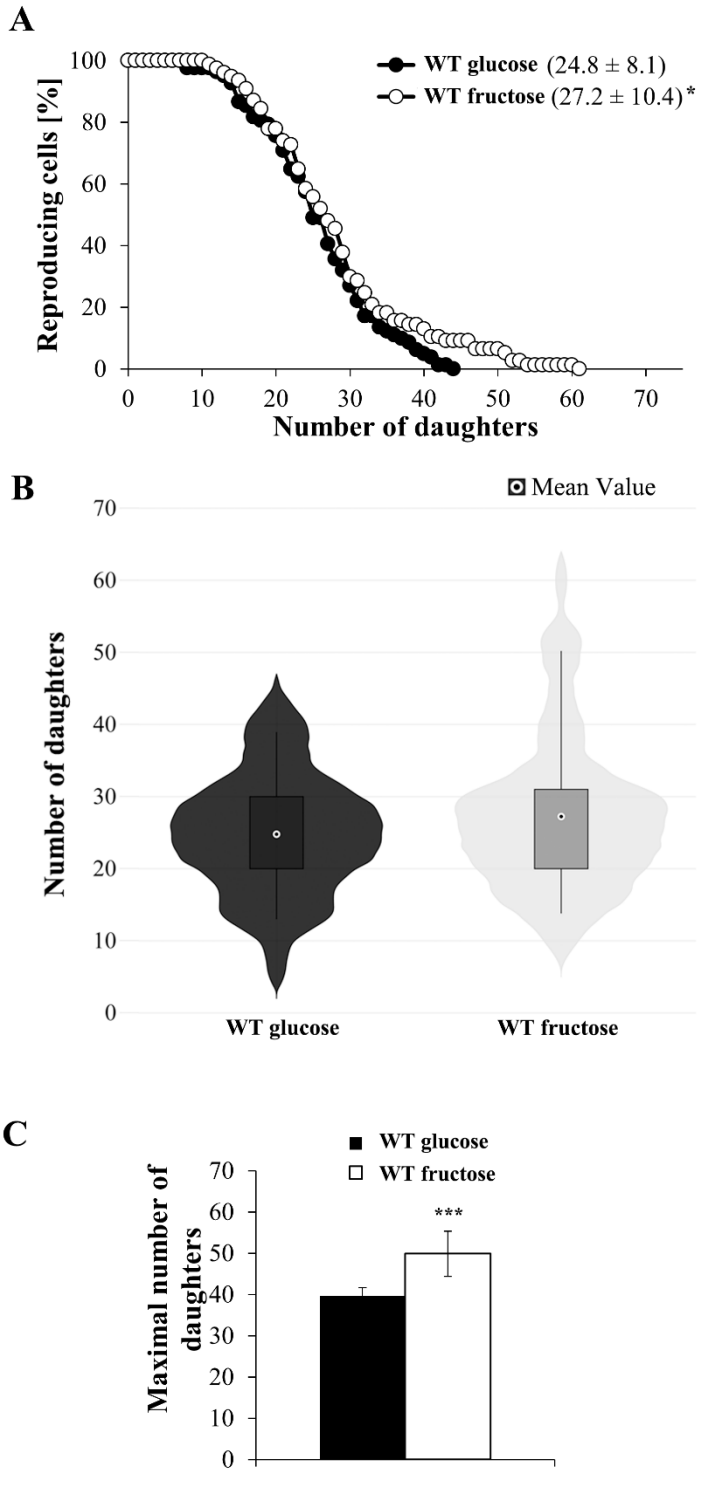
A
Reproducing cells [%]
100
80
60
40
20
0
0
10
20
30
40
50
60
70
Number of daughters
WT glucose (24.8 ± 8.1)
WT fructose (27.2 ± 10.4)*
B
Mean Value
Number of daughters
70
60
50
40
30
20
10
0
WT glucose
WT fructose
C
WT glucose
WT fructose
Maximal number of daughters
70
60
50
40
30
20
10
0
***

Figure 2

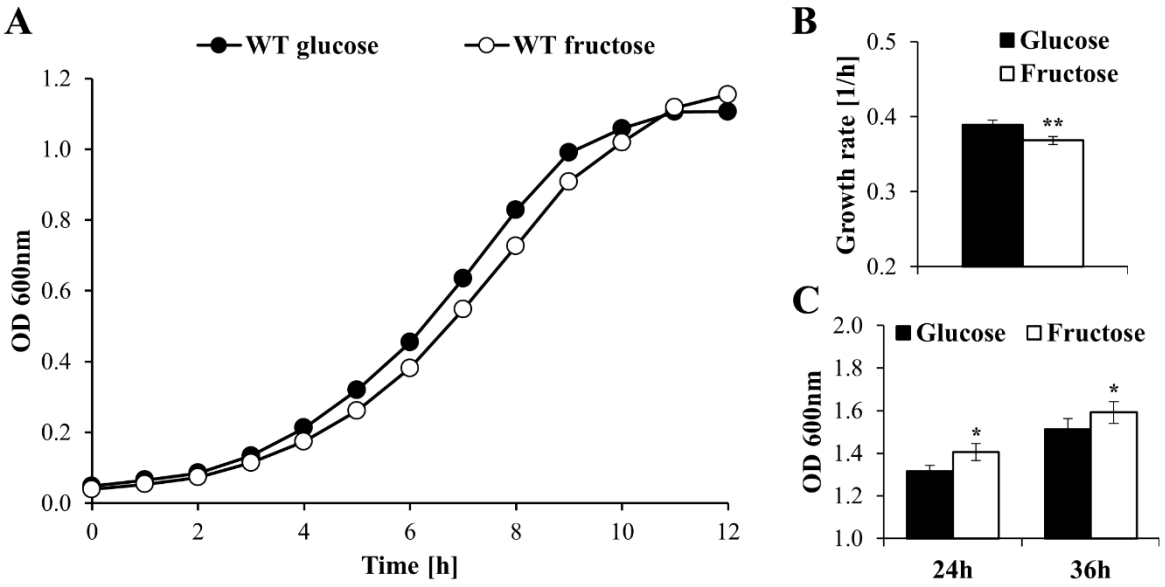
A
WT glucose
WT fructose
OD 600nm
Time [h]
B
Glucose
Fructose
Growth rate [1/h]
**
C
Glucose
Fructose
OD 600nm
24h
36h
*
*

Figure 3

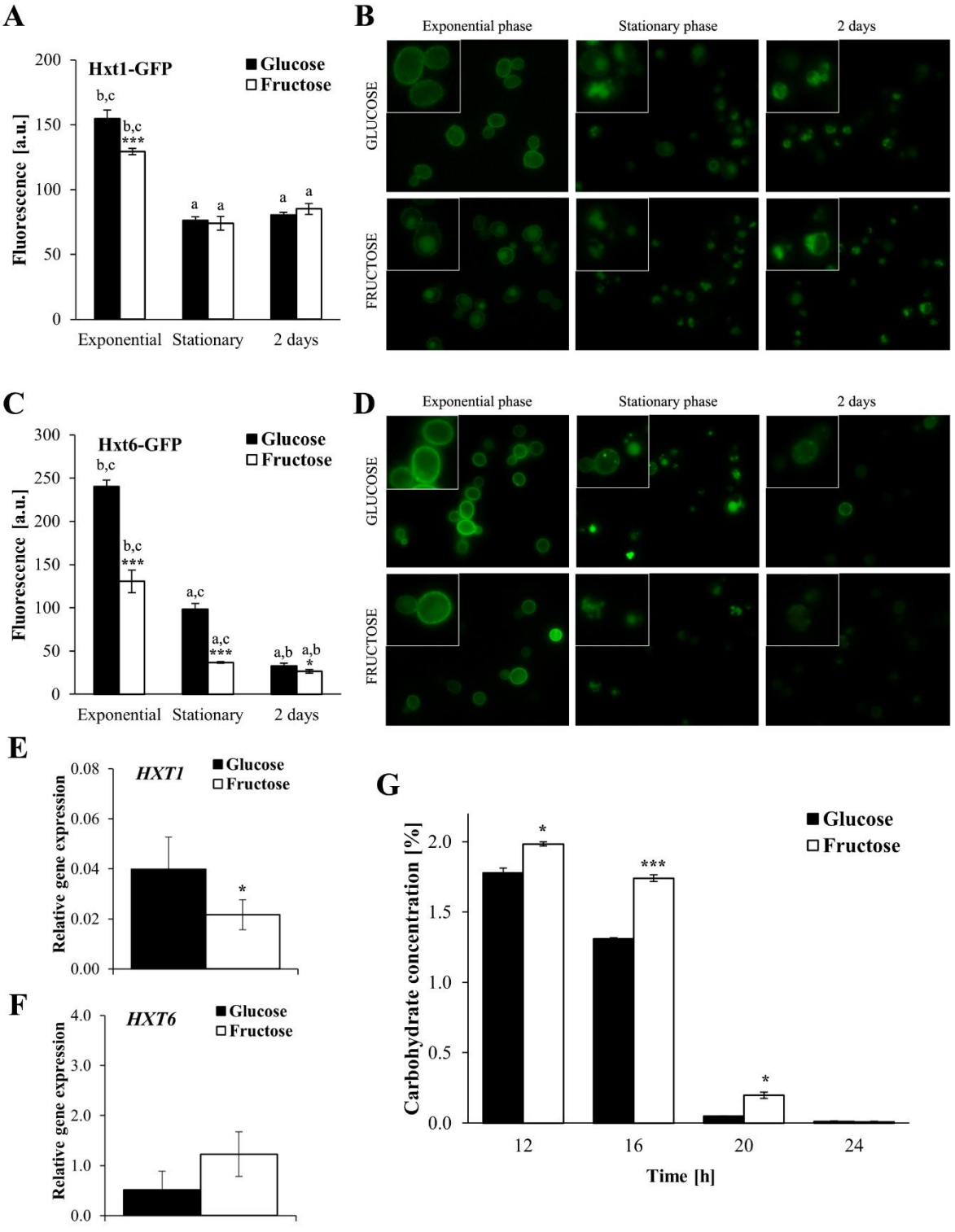
A
Hxt1-GFP
Glucose
Fructose
Fluorescence [a.u.]
200
150
100
50
0
b,c
b,c
***
a
a
a
a
Exponential
Stationary
2 days
B
Exponential phase
Stationary phase
2 days
GLUCOSE
FRUCTOSE
C
Hxt6-GFP
Glucose
Fructose
Fluorescence [a.u.]
300
250
200
150
100
50
0
b,c
b,c
***
a,c
a,c
***
a,b
a,b
*
Exponential
Stationary
2 days
D
Exponential phase
Stationary phase
2 days
GLUCOSE
FRUCTOSE
E
HXT1
Glucose
Fructose
Relative gene expression
0.08
0.06
0.04
0.02
0.00
*
F
HXT6
Glucose
Fructose
Relative gene expression
4.0
3.0
2.0
1.0
0.0
G
Glucose
Fructose
Carbohydrate concentration [%]
2.0
1.5
1.0
0.5
0.0
*
***
*
12
16
20
24
Time [h]

Figure 4

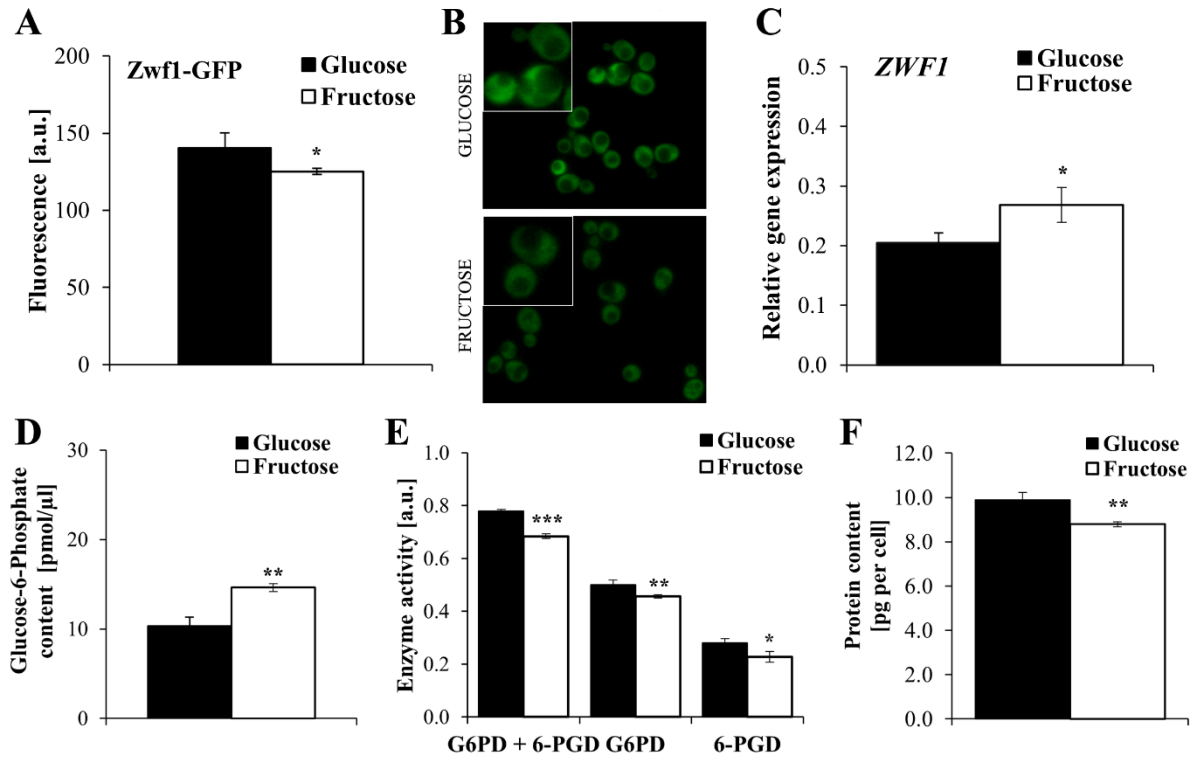
A
Zwf1-GFP
Glucose
Fructose
Fluorescence [a.u.]
200
150
100
50
0
*
B
GLUCOSE
FRUCTOSE
C
ZWF1
Glucose
Fructose
Relative gene expression
0.5
0.4
0.3
0.2
0.1
0.0
*
D
Glucose
Fructose
Glucose-6-Phosphate content [pmol/µl]
30
20
10
0
**
E
Glucose
Fructose
Enzyme activity [a.u.]
1.0
0.8
0.6
0.4
0.2
0.0
***
**
*
G6PD + 6-PGD
G6PD
6-PGD
F
Glucose
Fructose
Protein content [pg per cell]
12.0
10.0
8.0
6.0
4.0
2.0
0.0
**

Figure 5

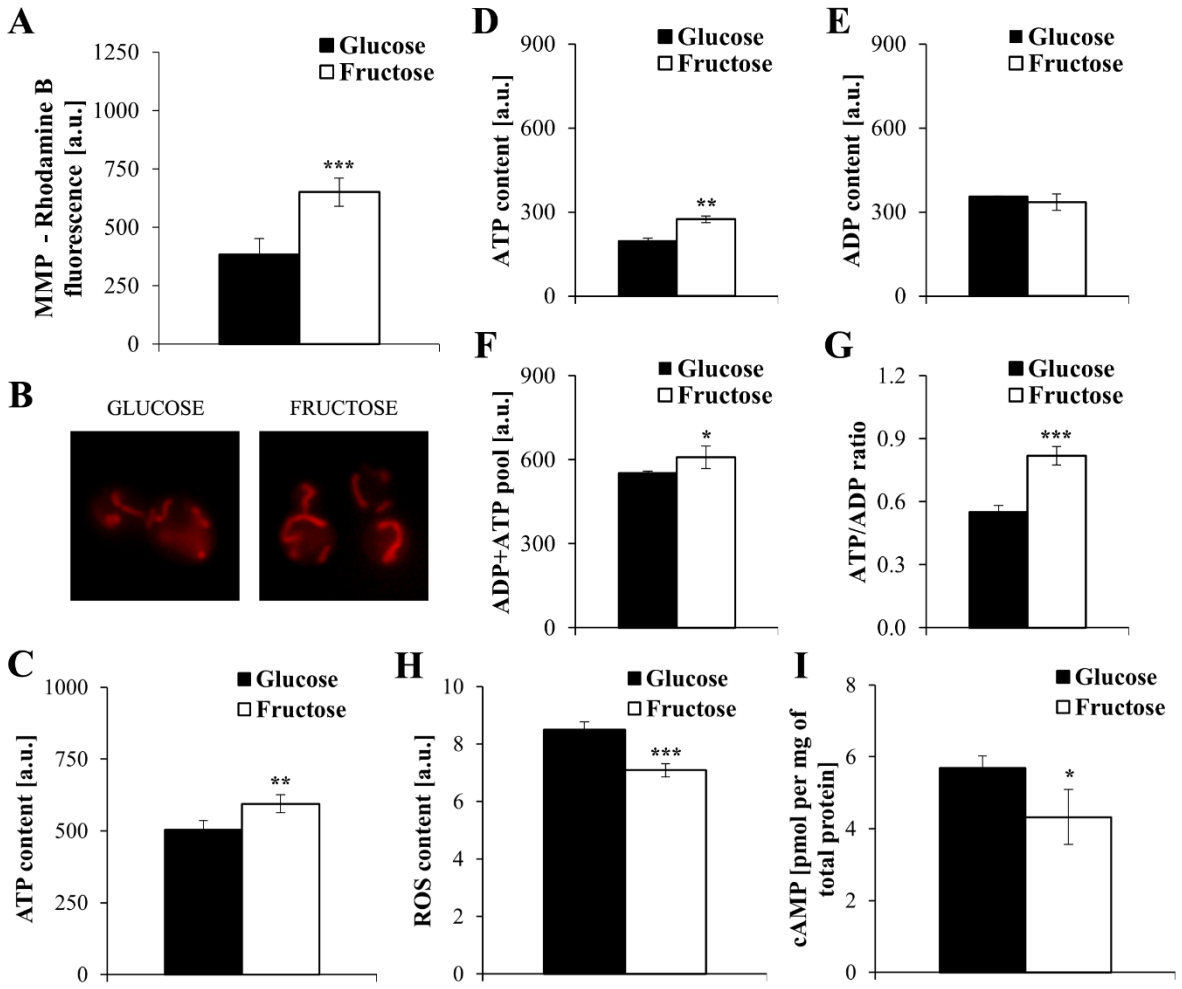
A
MMP - Rhodamine B fluorescence [a.u.]
1250
1000
750
500
250
0
Glucose
Fructose
***
B
GLUCOSE
FRUCTOSE
C
ATP content [a.u.]
1000
750
500
250
0
Glucose
Fructose
**
D
ATP content [a.u.]
900
600
300
0
Glucose
Fructose
**
E
ADP content [a.u.]
900
600
300
0
Glucose
Fructose
F
ADP+ATP pool [a.u.]
900
600
300
0
Glucose
Fructose
*
G
ATP/ADP ratio
1.2
0.9
0.6
0.3
0.0
Glucose
Fructose
***
H
ROS content [a.u.]
10
8
6
4
2
0
Glucose
Fructose
***
I
cAMP [pmol per mg of total protein]
8
6
4
2
0
Glucose
Fructose
*

Figure 6

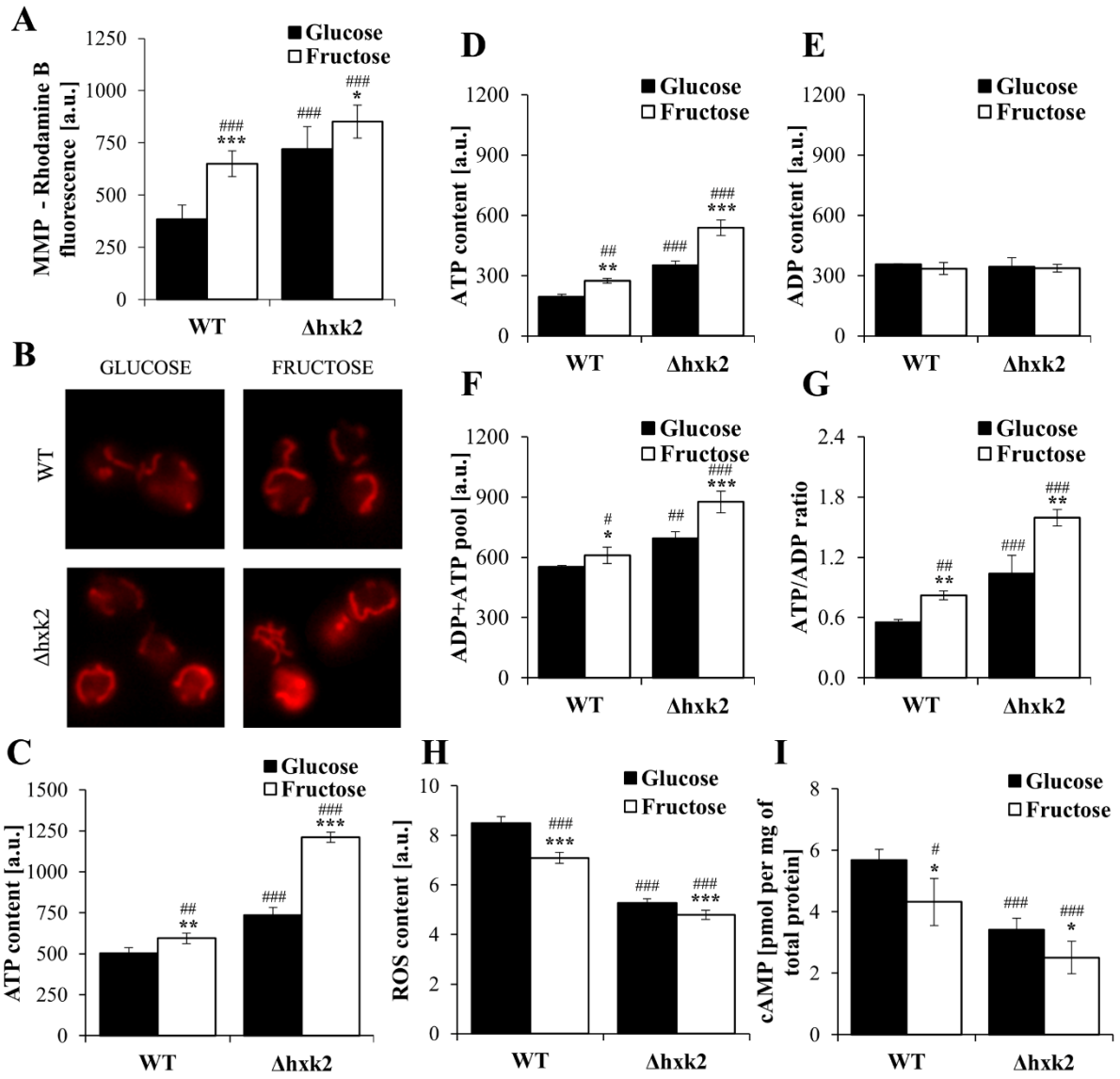
A
MMP - Rhodamine B fluorescence [a.u.]
Glucose
Fructose
WT
Δhxk2
B
GLUCOSE
FRUCTOSE
WT
Δhxk2
C
ATP content [a.u.]
D
ATP content [a.u.]
E
ADP content [a.u.]
F
ADP+ATP pool [a.u.]
G
ATP/ADP ratio
H
ROS content [a.u.]
I
cAMP [pmol per mg of total protein]

Figure 7

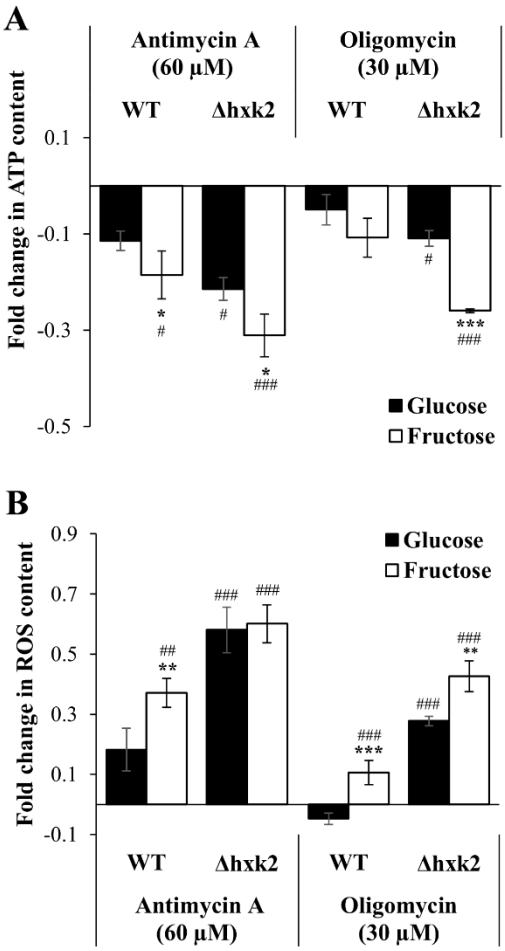
A
Antimycin A
(60 µM)
Oligomycin
(30 µM)
WT
Δhxk2
WT
Δhxk2
Fold change in ATP content
0.1
-0.1
-0.3
-0.5
Glucose
Fructose
B
Fold change in ROS content
0.9
0.7
0.5
0.3
0.1
-0.1
Glucose
Fructose
WT
Δhxk2
WT
Δhxk2
Antimycin A
(60 µM)
Oligomycin
(30 µM)

Figure 8

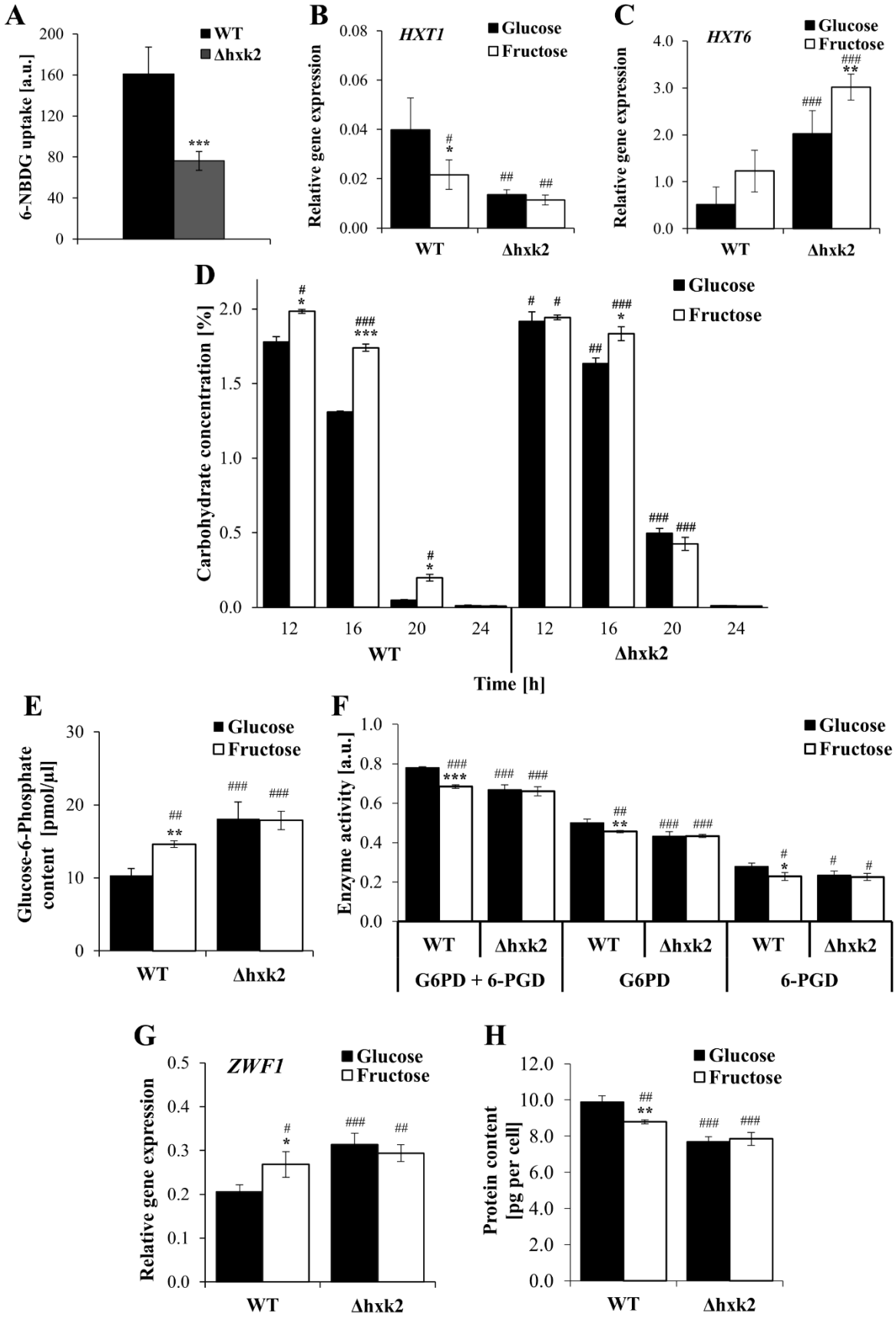
A
6-NBDG uptake [a.u.]
WT
Δhxk2
B
HXT1
Relative gene expression
Glucose
Fructose
WT
Δhxk2
C
HXT6
Relative gene expression
Glucose
Fructose
WT
Δhxk2
D
Carbohydrate concentration [%]
Glucose
Fructose
Time [h]
WT
Δhxk2
E
Glucose-6-Phosphate content [pmol/µl]
Glucose
Fructose
WT
Δhxk2
F
Enzyme activity [a.u.]
Glucose
Fructose
WT
Δhxk2
G6PD + 6-PGD
G6PD
6-PGD
G
ZWF1
Relative gene expression
Glucose
Fructose
WT
Δhxk2
H
Protein content [pg per cell]
Glucose
Fructose
WT
Δhxk2

Figure 9

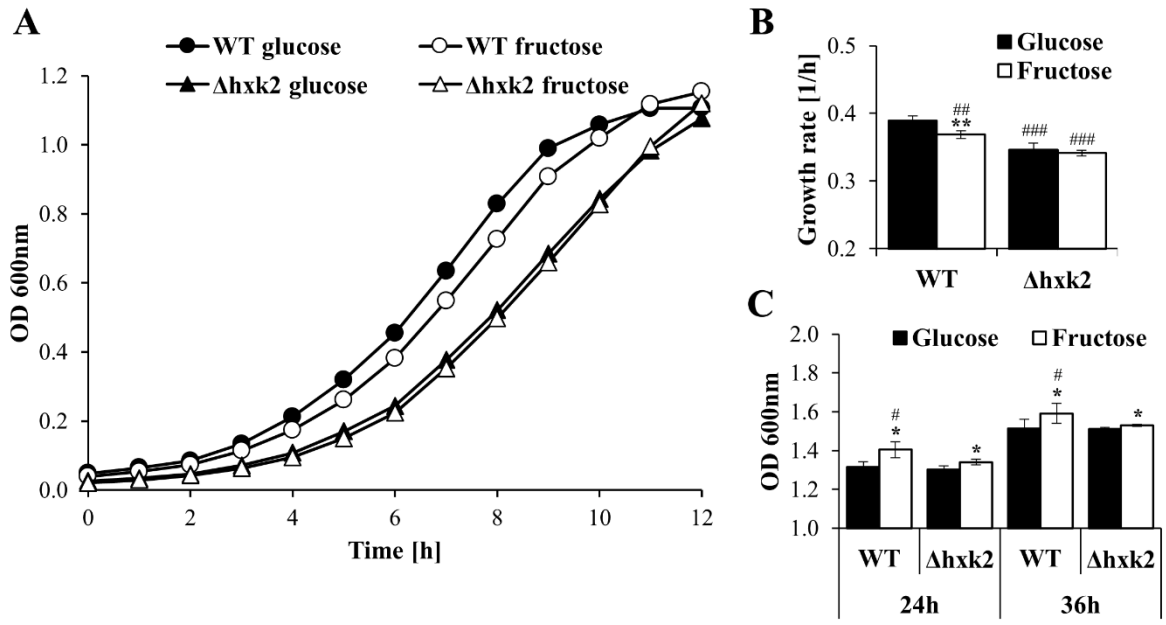
A
WT glucose
WT fructose
Δhxk2 glucose
Δhxk2 fructose
OD 600nm
Time [h]
B
Glucose
Fructose
Growth rate [1/h]
WT
Δhxk2
C
Glucose
Fructose
OD 600nm
WT
Δhxk2
WT
Δhxk2
24h
36h

Figure 10

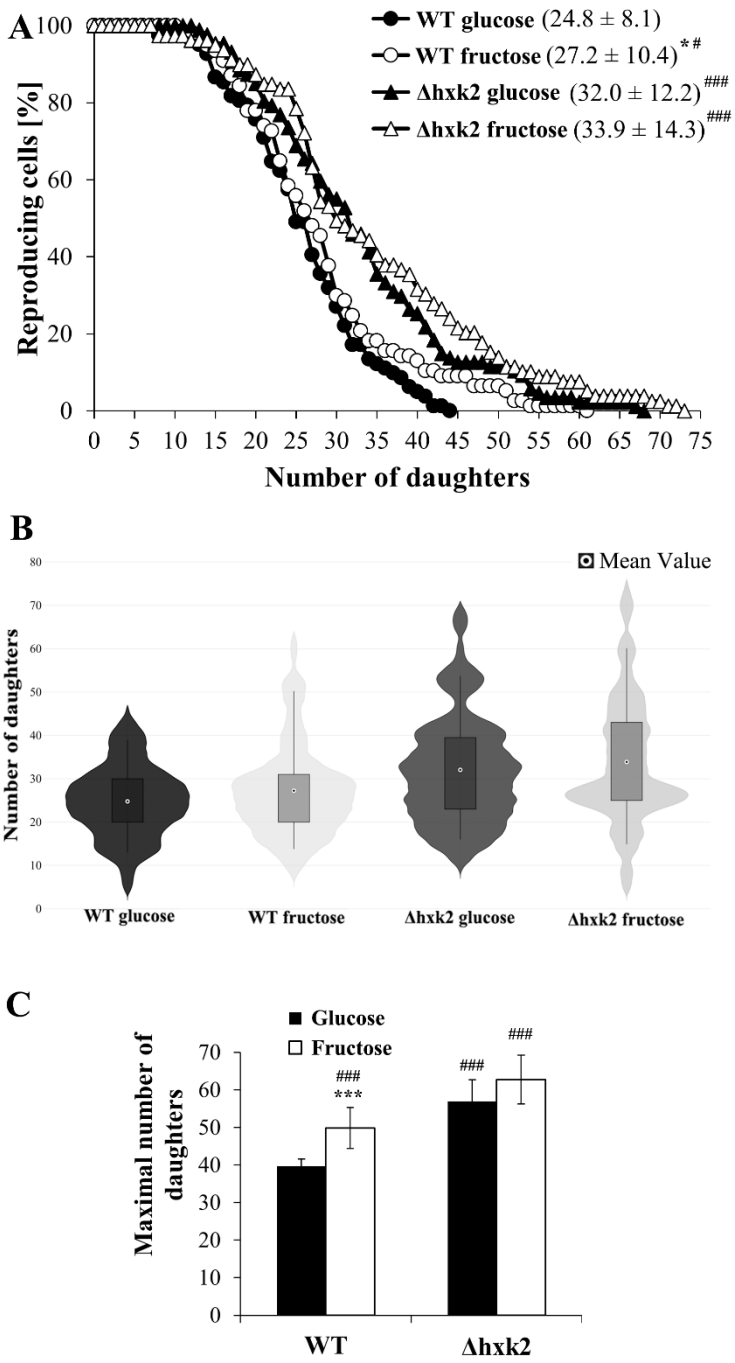
A
Reproducing cells [%]
Number of daughters
WT glucose (24.8 ± 8.1)
WT fructose (27.2 ± 10.4) *#
Δhxk2 glucose (32.0 ± 12.2) ###
Δhxk2 fructose (33.9 ± 14.3) ###
B
Mean Value
Number of daughters
WT glucose
WT fructose
Δhxk2 glucose
Δhxk2 fructose
C
Glucose
Fructose
Maximal number of daughters
###
***
###
###
WT
Δhxk2

Suplementary Figure 1

Strain / Cultivation time	Hxt1-GFP		Hxt6-GFP		Zwf1-GFP	
	Carbohydrate concentration [%]					
	Glucose	Fructose	Glucose	Fructose	Glucose	Fructose
Exponential	**1.47** ± *0.09*	**1.82** ± *0.06*	**1.23** ± *0.01*	**1.82** ± *0.01*	**1.20** ± *0.04*	**1.81** ± *0.01*
Stationary	**0.04** ± *0.00*	**0.03** ± *0.00*	**0.04** ± *0.00*	**0.03** ± *0.00*	**0.04** ± *0.00*	**0.03** ± *0.00*
2 days	**0.01** ± *0.00*	**0.00** ± *0.00*	**0.01** ± *0.00*	**0.00** ± *0.00*	**0.01** ± *0.00*	**0.00** ± *0.00*

Suplementary Figure 2